19

Anatomy and Relationships of *Bolong yixianensis,* an Early Cretaceous Iguanodontoid Dinosaur from Western Liaoning, China

Wu Wenhao* and Pascal Godefroit

The skeleton (YHZ-001) of a new basal iguanodontoid was discovered in the middle part of the Yixian Formation in western Liaoning, China. *Bolong yixianensis* Wu, Godefroit, and Hu, 2010, is characterized by cranial, dental, and postcranial autapomorphies, as well as a unique combination of characters. A phylogenetic analysis reveals that *Bolong* is the most primitive Hadrosauroidea described so far. During the Lower Cretaceous, Iguanodontoidea were subdivided into Iguanodontidae, which mainly occupied Neopangean territories, and Hadrosauroidea in Asia. The presence of Iguanodontoidea in the middle part of the Yixian Formation indicates that connections between Asia and western North America and/or Europe were already established during or before the Barremian.

19.1. A, *Bolong yixianensis,* YHZ-001 (holotype). Skull and partially articulated postcranial skeleton, as discovered, in right lateral view. *Abbreviations:* L, left; R, right. B, Skull reconstruction in left lateral view.

Introduction

Iguanodontoidea (=Hadrosauriformes sensu Sereno, 1997) is defined as *Iguanodon*, *Parasaurolophus*, their most recent common ancestor, and all descendants (Sereno, 1998, amended). During the Early Cretaceous, iguanodontoids had achieved a pan-Laurasian distribution and were also represented in Africa (Norman, 2004). During the Upper Cretaceous, advanced Iguanodontoidea, or Hadrosauridae (a node-based taxon defined as the most recent common ancestor of *Bactrosaurus* and *Parasaurolphus*, plus all the descendants of this common ancestor; see Norman, 2004, fig. 11.22), replaced basal iguanodontoids and became the most diverse and abundant large vertebrates of Laurasia during the Campanian and the Maastrichtian.

Many new basal iguanodontoids were described during the 2000s, most of which have been recovered from Early Cretaceous deposits in China and Mongolia, including *Altirhinus kurzanovi*, from Khuren Dukh (late Aptian–Early Albian) of Mongolia (Norman, 1998), *"Probactrosaurus" mazongshanensis* and *Equijubus normani*, from the Ximinbao Group (Aptian–Albian) of Gansu province (Lü, 1997; You et al., 2003b), *Jintasaurus meniscus*, from the Xinminpu Group (?Albian) of Gansu province (You and Li, 2009), *Nanyangosaurus zhugeii*, from the Sangping Formation (?Albian) of Henan province (Xu et al., 2000), and *Penelopognathus weishampeli*, from the Bayan Gobi Formation (Albian, Lower Cretaceous) of Inner Mongolia (Godefroit et al., 2005). *Lanzhousaurus magnidens*, represented by an incomplete skeleton from the Hekou Group (Early Cretaceous) of Gansu province, may represent a more basal iguanodontian (You et al., 2005).

The Early Cretaceous Jehol Biota of western Liaoning province in China is famous for its abundant, extraordinarily diversified, and exquisitely preserved fossils. The dinosaur fauna of the Jehol Biota is dominated by small-bodied taxa (<3 m in body length), including a variety of coelurosaurian theropods, basal ceratopsians, the basal ornithopods *Jeholosaurus,* and the ankylosaur *Liaoningosaurus* (Xu and Norell, 2006; Zhou, 2006). Larger herbivorous dinosaurs are rare in the Jehol fauna and include the titanosauriform *Dongbutitan dongi* (Wang et al., 2007) and the basal iguanodontoid *Jinzhousaurus yangi* (Wang and Xu, 2001; Barrett et al., 2009; Wang et al., 2011). *Shuangmiaosaurus gilmorei*, on the basis of an incomplete and deformed skull, was also collected in western Liaoning province, but in the younger Sunjiawan Formation (late Early or early Late Cretaceous; You et al., 2003a).

Here we describe the skeleton of a new basal iguanodontoid collected in 2000 in the middle part of the Yixian Formation to supplement the initial report by Wu et al. (2010). The fossil site is located at Bataigou, Toutai county. This incomplete skeleton was fossilized lying on its left flank, with the limbs roughly perpendicular to the vertebral column and parallel to each other, and with the skull and neck retracted over the back (Fig. 10.1). The estimated length for the complete skeleton (the tip of the tail is missing) is ~4 m (smaller than the holotype of *Jinzhousaurus*, which is 5–5.5 m). For the sake of convenience, all nonhadrosaurid Iguanodontoidea will be termed "basal iguanodontoids" hereafter.

Comparisons are made to other Iguanodontia on the basis of published descriptions of *Tenontosaurus* spp. (Ostrom, 1970; Forster, 1990; Winkler et al., 1997), *Dryosaurus* spp. (Janensch, 1955; Galton, 1983), *Zalmoxes* spp. (Weishampel et al., 2003; Godefroit et al., 2009), *Camptosaurus dispar* (Gilmore, 1909; Erickson, 1988), *Iguanodon bernissartensis* (Norman, 1980), *Mantellisaurus atherfieldensis* (Norman, 1986), *Ouranosaurus nigeriensis* (Taquet, 1976), *Lanzhousaurus magnidens* (You et al., 2005), *Lurdusaurus arenatus* (Taquet and Russell, 1999), *Nanyangosaurus zhugeii* (Xu et al. 2000), *Jinzhousaurus yangi* (Barrett et al., 2009), *Equijubus normani* (You et al., 2003b), *Altirhinus kurzanovi* (Norman, 1998), *Penelopognathus weishampeli* (Godefroit et al., 2005), *Fukuisaurus tetoriensis* (Kobayashi and Azuma, 2003), *Probactrosaurus gobiensis* (Norman, 2002), "*Probactosaurus*" *mazongshanensis* (Lü, 1997), *Eolambia caroljonesa* (Kirkland, 1998), *Protohadros byrdi* (Head, 1998), *Bactrosaurus johnsoni* (Gilmore, 1933; Godefroit et al., 1998), *Levnesovia transoxiana* (Sues and Averianov, 2009), *Shuangmiaosaurus gilmorei* (You et al., 2003a), *Tethyshadros insularis* (Dalla Vecchia, 2009), *Telmatosaurus transsylvanicus* (Weishampel et al., 1993), and various Euhadrosauria. *Jintasaurus meniscus* You and Li, 2009, was published after the completion of this chapter and has not been included in the analysis.

Systematic Paleontology

Dinosauria Owen, 1842
Ornithischia Seeley, 1887
Ornithopoda Marsh, 1881
Iguanodontia Dollo, 1888 [Sereno, 1986]
Iguanodontoidea Cope, 1869
Hadrosauroidea Cope, 1869

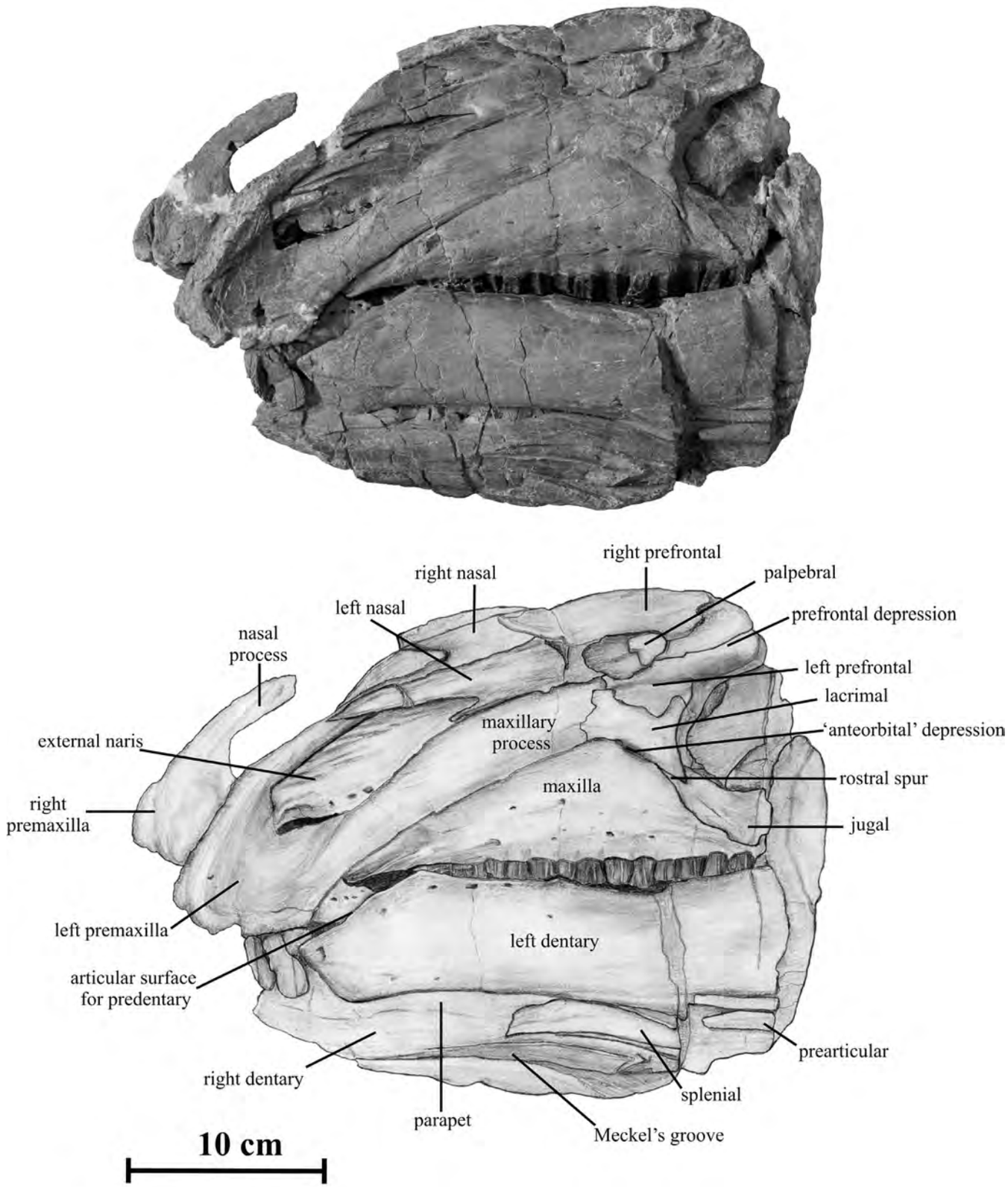

19.2. *Bolong yixianensis,* YHZ-001 (holotype). Rostral portion of the skull in left lateral view.

Bolong yixianensis Wu, Godefroit, and Hu, 2010
(Figs. 19.1–19.11)

Etymology. The generic name is in honor of Bo Haichen and Bo Xue, who discovered and excavated the holotype; *long* means "dragon" in Chinese. The specific name refers both to the Yixian Formation, where the holotype was discovered, and to the city of Yixian, where the holotype is housed and displayed.

Holotype. YHZ-001, housed in Yizhou Fossil Museum, Yixian City, Liaoning province (P.R. China).

Locality and horizon. Bataigou, Toutai, Yixian County, western Liaoning province, P.R. China. GPS coordinates: N41°36'6.79", E121°7'43.1". Dakangpu Member (equivalent to the Dawangzhangzi Beds) of the middle part of Yixian Formation, Late Barremian–Early Aptian (Smith et al., 1995; Swisher et al., 1999, 2002).

Diagnosis. Differs from all other iguanodontoid taxa in possessing the following autapomorphies: depressed area at the junction between maxilla and lacrimal, corresponding to the position of the antorbital fenestra in *Iguanodon*, *Mantellisaurus*, and *Ouranosaurus*; caudal ramus of prefrontal forming a rostrocaudally depressed area above the orbital margin; ventral process of predentary extending caudally parallel to the ventral margin of the predentary main body; rostrodorsal articular surface for the predentary occupying less than two-thirds of the height of the rostral part of the dentary and rostral tip of dentary therefore situated above the ventral third of the bone; primary ridge deflected distally on maxillary crowns; ulna and radius proportionally short and robust (ratio craniocaudal height of proximal part/length = 0.28 for ulna and 0.33 for radius); proximal and distal ends of radius nearly symmetrically enlarged craniocaudally and triangular in medial and lateral views; postacetabular process of ilium dorsoventrally narrow (ratio length/maximal height = 2); metatarsals proportionally short: ratio metatarsal III/femur = 0.18.

Description:

All the measurements taken on YHZ-001 are compiled in Appendix 19.1.

The preorbital region of the skull is well preserved, and both sides were prepared. Like the rest of the skeleton, it was laterally crushed during fossilization. Bones are usually preserved in natural connection on the left side of the skull (Fig. 19.2), in direct contact with the sediment after the death of the animal, whereas they were slightly displaced on the right side of the skull (Fig. 19.3). A fault bisects the skull, and the fronto-orbital region of the skull has consequently been lost. Only the right side of the back of the skull has been prepared (Fig. 19.4), but this region is crushed and poorly preserved.

External naris. The external naris is drop shaped and proportionally larger (45% of preorbital length) than in *Jinzhousaurus* (38%), *Iguanodon*, *Mantellisaurus* (approximately 28–30%), and *Ouranosaurus* (approximately 18%). However, it is proportionally much shorter than in *Altirhinus* (approximately 56%) and Hadrosauridae. The maximum height of the external naris is located at the level of the rostral tip of the maxilla (Fig. 19.2).

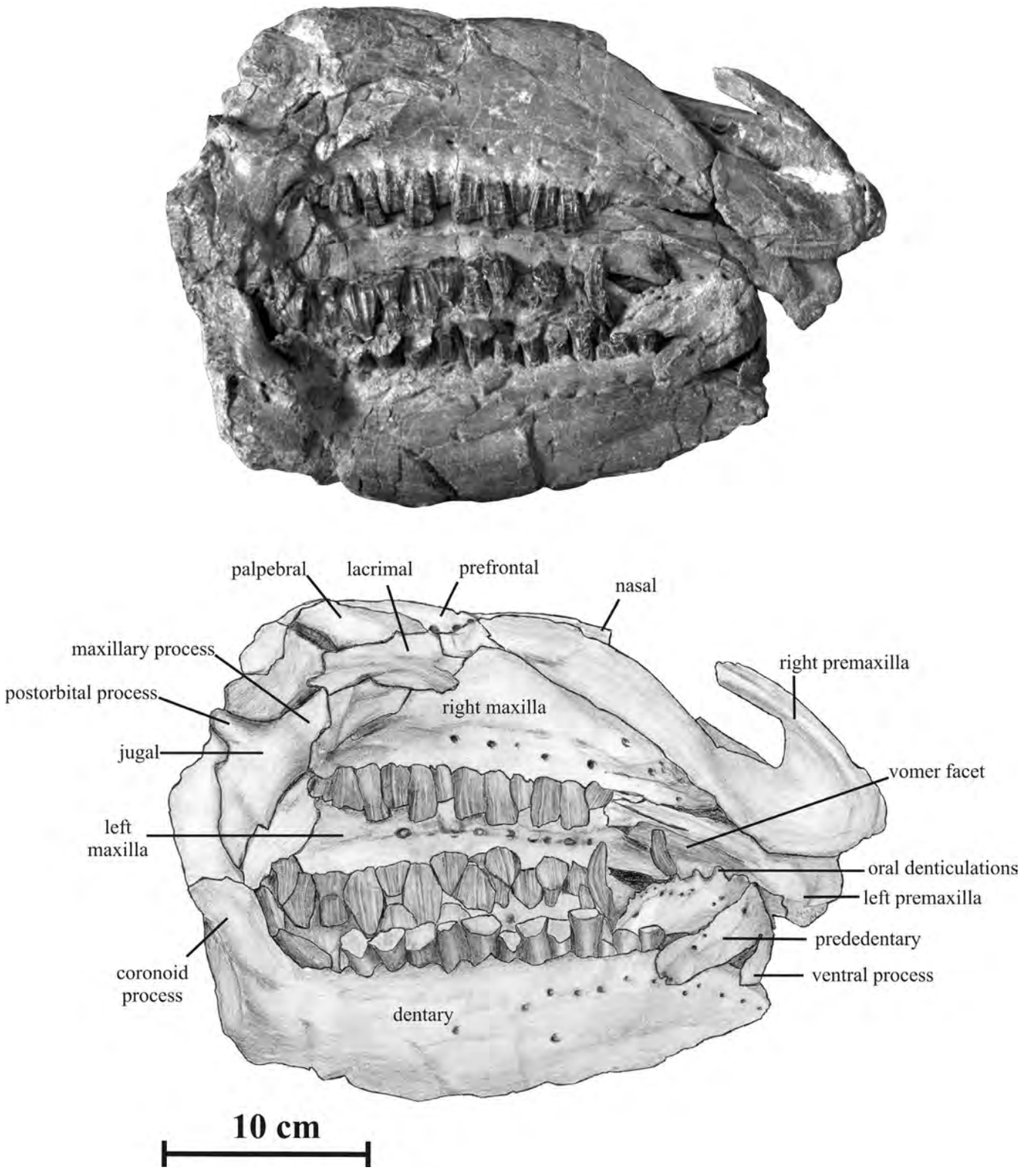

19.3. *Bolong yixianensis,* YHZ-001 (holotype). Rostral portion of the skull in right lateral view.

Nasal. Both nasals are preserved (Fig. 19.2). These elongated straplike elements are slightly arched in lateral view. The external surface of the nasal is gently convex, whereas its internal surface is concave. Rostrally, the nasal divides into two processes: an elongated rostromedial process that forms the longest part of the dorsal margin of the external naris and a small subtriangular rostrolateral process that forms the caudal fifth of the ventral margin of the external naris. Therefore, the caudal corner of the external naris is entirely circumscribed by the nasal in *Bolong*. The rostrolateral process is developed in *Jinzhousaurus* but absent in *Iguanodon*, *Mantellisaurus*, *Ouranosaurus*, *Equijibus*, and *Altirhinus* (contra Barrett et al., 2009). It is developed in some hadrosaurines, including *Gryposaurus* spp. and *Brachylophosaurus canadensis* (Gates and Sampson, 2007). Rostrally, the ventral margin of the nasal is grooved where it contacted the maxillary process of the premaxilla. There is apparently no contact between the nasal and the lacrimal, contrary to the situation observed in *Ouranosaurus* and *Altirhinus*. The articulation with the prefrontal is extensive on the caudolateral margin of the nasal, but the caudal part of the nasals is too crushed and deformed to be adequately described.

Premaxilla. The oral margin of the premaxilla extends well below the level of the maxillary tooth row (Fig. 19.2). Its external margin is slightly everted, as occurs in many other basal iguanodontoids (e.g., *Iguanodon*, *Mantellisaurus*, *Jinzhousaurus*, *Equijubus*, and *Probactrosaurus*). The rostral part of the oral margin is thickened and rugose, indicating that it was covered by a keratinous ramphotheca in life (Ostrom, 1961). Above this area, the external surface of the premaxilla is obliquely depressed and forms a narrow internarial septum that leads caudally into the narial chamber. Two small foramina are positioned close to the rostral margin of the internarial septum. The nasal process is gently curved and participates in the rostrodorsal margin of the external naris. It is mediolaterally compressed. Its external surface has an elongated articular surface covered by the rostromedial process of the nasal. Its medial surface is perfectly flat where it contacted the nasal process of the paired premaxilla. The lateral surface of the maxillary process is straight and planar. Rostrally, it is separated from the narial fossa by a blunt oblique ridge. Its ventromedial margin contacts the maxilla along its whole length. Its dorsal border floors the external naris. It reaches its maximum dorsoventral depth at the level of the caudal corner of the external naris and forms a thin sheet along the side of the snout between the nasal and the maxilla. This is similar to the condition seen in *Jinzhousaurus*, *Altirhinus*, *Eolambia*, *Ouranosaurus*, and *Probactrosaurus*, but contrasts with that seen in other basal iguanodontoids (e.g., *Iguanodon*, *Mantellisaurus*, and *Equijubus*), in which the maxillary process is much more slender and tapers distally (Barrett et al., 2009). The thin caudal part of the maxillary process covers the lacrimal and apparently contacts the prefrontal along a short distance. This contact, excluding the lacrimal from the nasal, appears more extensive in *Iguanodon*, *Mantellisaurus*, *Jinzhousaurus*, and, to a lesser extent, in *Equijubus*.

Maxilla. As usual in basal iguanodontoids, the maxilla is shaped like a low isosceles triangle in lateral view (Figs. 19.2–19.3). There are 15 tooth columns. The apex of the maxilla is caudal to the center of the bone, located at the level of the 10th tooth row. Rostrally, the maxilla is wedge shaped,

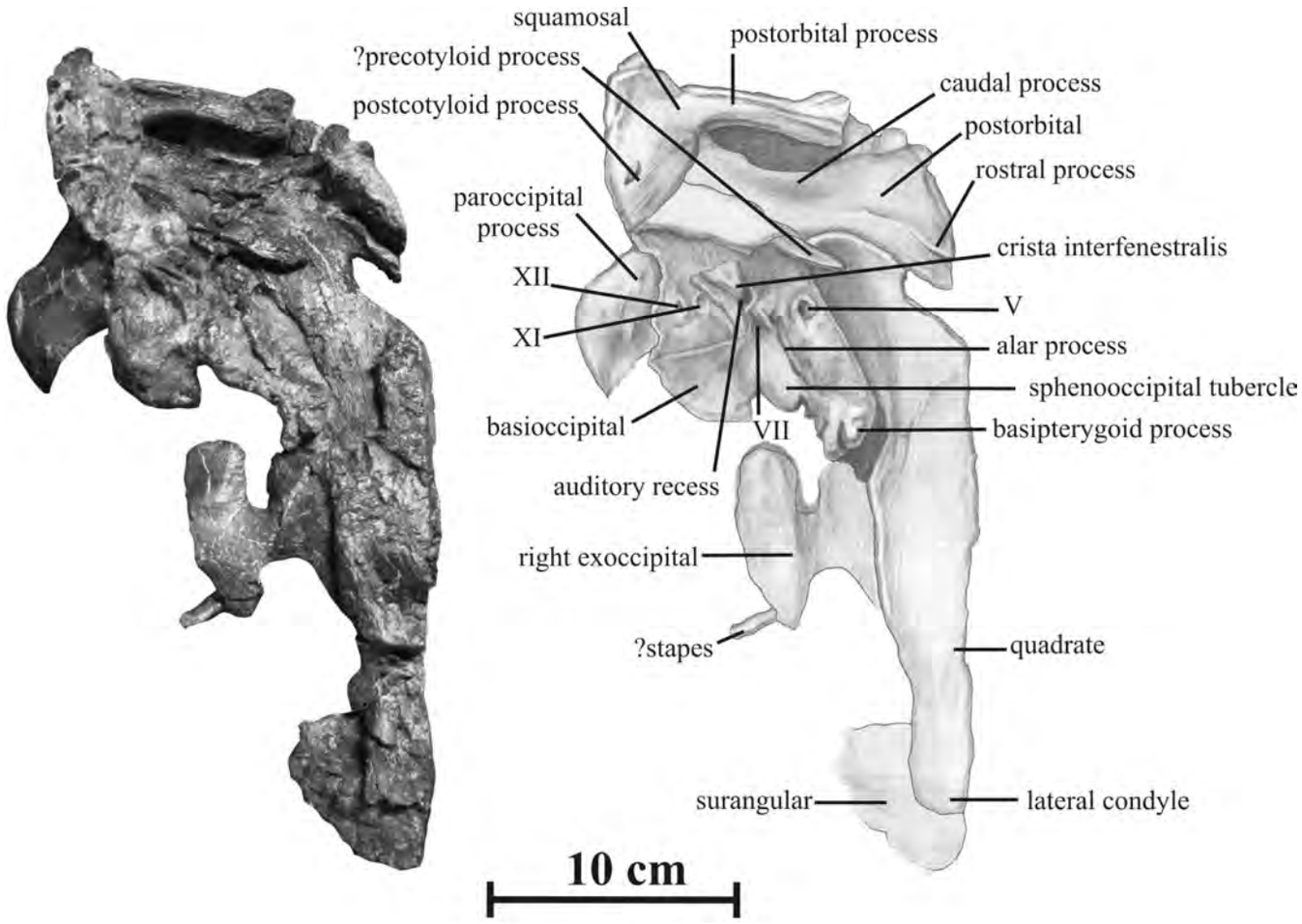

19.4. *Bolong yixianensis,* YHZ-001 (holotype). Caudal portion of the skull in right lateral view.

but its rostral tip is less distinctly downturned than in *Jinzhousaurus*, *Altirhinus*, *Equijubus*, *Shuangmiaosaurus*, and *Protohadros*. However, this character cannot easily be quantified phylogenetically. The dorsal surface of this rostral end forms an oblique dorsolaterally directed flange against which articulates the maxillary process of the premaxilla. The caudodorsal articulation with the lacrimal is much longer than in *Jinzhousaurus* and extends rostrally to the apex of the maxilla. There is no evidence for an antorbital opening, but a depressed area is present at the junction between the lacrimal and the maxilla, just caudal to the apex of the latter bone (Fig. 19.2). This depression, absent in *Jinzhousaurus*, *Equijubus*, and *Altirhinus*, corresponds to the emplacement of the antorbital opening in the basal iguanodontoids *Iguanodon*, *Mantellisaurus*, and *Ouranosaurus*. The lateral side of the maxilla is gently convex dorsoventrally, contrasting with the situation observed in *Jinzhousaurus* and *Equijubus*, in which a well-developed, acute, and rostrocaudal ridge defines the dorsal boundary of a deep buccal emargination (You et al., 2003b, fig. 1; Barrett et al., 2009). In *Bolong*, the slight buccal emargination is limited dorsally by six elliptical foramina. The dorsal part of the lateral surface is also pierced by six irregularly distributed foramina, mainly concentrated on the rostral half of the maxilla. The foramina are not as numerous and large as in *Jinzhousaurus* (Barrett et al., 2009) and particularly in *Equijubus* (You et al., 2003b). A hooklike jugal process, similarly developed in *Iguanodon*, *Mantellisaurus*, *Ouranosaurus*,

Jinzhousaurus, *Altirhinus*, *Probactrosaurus*, and *Bactrosaurus*, projects ventrolaterally and caudally. The jugal process is absent or poorly developed in *Equijubus* (You et al., 2003b) and *Fukuisaurus* (Kobayashi and Azuma, 2003). At its rostral end, the dorsomedial border of the maxilla forms a quite elongated and rugose sutural surface for the vomer (Fig. 19.3).

Lacrimal. This bone is rectangular and rostrocaudally elongate in *Bolong*, extending in front of the apex of the maxilla (Fig. 19.2). It is rather thick caudally, where it participates in the rostral margin of the orbit. It forms a robust caudoventral process that contacts the rostral process of the jugal. At this level, its lateral side is pierced by a small foramen at approximately midheight. It extends rostrally as a thin sheet of bone between the maxilla, the premaxilla, and the prefrontal. The right lacrimal was displaced during fossilization (Fig. 19.3). The caudal part of its ventral margin is strongly arched, corresponding to the dorsal margin of the antorbital fenestra in *Mantellisaurus* (Norman, 1986, fig. 12). More rostrally, the ventral margin has a bevelled and elongate contact for the maxilla. In *Jinzhousaurus*, the lacrimal is triangular in shape and more reduced than in *Bolong*.

Prefrontal. In lateral view, the prefrontal is crescentic in outline. Its dorsal margin has a straight contact with the nasal along its whole length. The caudal ramus of the prefrontal, which forms the rostrodorsal portion of the orbital margin, is particularly robust. Around the orbital margin, it forms a thickened ridge. Above this ridge, the lateral side of the caudal ramus forms a rostrocaudally elongate depression (Fig. 19.2). The rostral plate of the prefrontal is higher and much thinner mediolaterally. Ventrally, it overlaps the lacrimal. Its rostrodorsal corner apparently contacts the premaxilla. A roughened surface on the rostrolateral corner of the prefrontal forms the articular surface for the palpebral.

Palpebral (supraorbital). The palpebral of *Bolong* is robust. The rostral part of the left palpebral contacts the rostral ramus of the prefrontal (Fig. 19.2). It is slightly expanded and gently convex dorsoventrally.

Postorbital. The right postorbital is poorly preserved (Fig. 19.4). It is crushed inside the infratemporal fenestra and its rostral part is missing. The jugal process is robust, inclined rostrally and it tapers ventrally. The caudal process is thickened and straight along its whole length.

Squamosal. The right squamosal is poorly preserved (Fig. 19.4). The postorbital process is perfectly straight, particularly elongate, and dorsoventrally narrow. Its lateral side bears two prominent and parallel horizontal ridges that limit ventrally and dorsally an extended articular surface for the caudal process of the postorbital. The postcotyloid process appears triangular in lateral view and is relatively long, as in *Mantellisaurus* (Norman, 1986, fig. 14). The precotyloid process is tentatively identified as a thin straplike element displaced in the infratemporal fenestra.

Jugal. Both jugals are incompletely preserved. The maxillary process is proportionally shorter than in *Ouranosaurus* (Taquet, 1976, fig. 19) and *Equijibus* (You et al., 2003b). Rostrally, a small triangular projection from the maxillary process overlies the junction between the maxilla and the lacrimal (Fig. 19.2). This rostral spur is less developed than in *Altirhinus* (Norman, 1998, fig. 9). Above this projection, the dorsal side of the maxillary process forms an extended laterally facing articular facet for the

lacrimal. The robust postorbital process is incompletely preserved on the right side of the skull (Fig. 19.3); it forms a 110-degree angle with the maxillary process. At the junction between the maxillary and the postorbital processes, the main body of the jugal appears dorsoventrally higher than in *Jinzhousaurus*. Below the infratemporal fenestra, the ventral margin of the jugal is gently concave.

Quadrate. The right quadrate is completely crushed and its rostral part is missing. The quadrate is proportionally high and rostrocaudally narrow in lateral view (Fig. 19.4). Its caudal margin is regularly concave, so that it looks deflected caudally, as observed in numerous iguanodontoids including *Jinzhousaurus* (Wang and Xu, 2001). The distal end of the quadrate forms a large hemispherical lateral condyle that articulates with the surangular component of the mandibular glenoid.

Exoccipital. The left exoccipital is partially preserved in anatomical position. The right one is ventrally displaced between the quadrate and the cervical series (Fig. 19.4). The medial side of the exoccipital condyloid is visible, but crushed. Caudal to the strong crista tuberalis that extends the entire height of the condyloid, two large foramina probably represent the passages for the hypoglossal nerve rostrally (XII) and the accessory nerve (XI) caudally. Rostral to the oblique pillar, the wall of the braincase forms a wide and depressed auditory recess. An oblique crista interfenestralis divides the auditory recess into a rostral fenestra ovalis (stapedial recess) and a caudal metotic foramen. The paroccipital process is massive and projects ventrolaterally, reaching about the level of the base of the occipital condyle.

Basioccipital. The occipital condyle is massive and its articular surface is not perfectly vertical as in hadrosauroids, but oriented caudoventrally, as observed in the basal iguanodontoids *Iguanodon*, *Mantellisaurus*, and *Ouranosaurus*. A prominent pyriform facet on the dorsolateral side of the basioccipital marks the contact with the right exoccipital. The basal tubera are separated from the occipital condyle by a distinct neck.

Basisphenoid. The caudolateral aspect of the basisphenoid is visible (Fig. 19.4). In front of the basal tubera, the basipterygoid processes project well below the occipital condyle as in Hadrosauridae (Godefroit et al., 1998). In *Iguanodon*, *Mantellisaurus*, and *Ouranosaurus*, on the other hand, the distal end of the basipterygoid processes is nearly on the same horizontal plane as the ventral border of the occipital condyle. On the lateral wall of the basisphenoid, the alar process is found directly above the base of the basipterygoid process, from which it is distinctly separated.

Predentary. The predentary is laterally crushed (Fig. 19.3). Its oral border bears four pairs of conical projections, better developed than in *Jinzhousaurus*, which are replaced further laterally by a rounded ridge. The lateral edge borders a moderately developed lingual shelf, broader caudally than rostrally. Beneath the denticulate border, the bone is punctured by foramina and grooves associated with the attachment of a keratinous beak. The ventral surface of the predentary forms a shelf that fitted on the rostral edge of the dentary. A well-developed ventral process helped to secure the dentaries in position. The ventral process is clearly bifurcate, contrary to that of *Jinzhousaurus* (Barrett et al., 2009), and is perfectly parallel to the ventral margin of the predentary, embracing the depressed area along the rostroventral border of the dentary. The ventral process of the

19.5. *Bolong yixianensis,* YHZ-001 (holotype). A, Dentition. B, Right maxillary teeth. C, Left dentary teeth.

predentary is usually more vertical, ventrocaudally inclined, in other basal iguanodontoids, as observed in *Iguanodon*, *Mantellisaurus*, *Ouranosaurus*, *Jinzhousaurus*, and *Altirhinus*. The rostral surface of the predentary has two deep diagonal vascular grooves that connect the dorsolateral corner of the ventral process to the base of the median crenulation. These grooves are also well developed in *Iguanodon*, *Mantellisaurus*, *Ouranosaurus*, *Jinzhousaurus*, *Altirhinus*, *Probactrosaurus*, and *Protohadros*.

Dentary. Both dentaries are preserved in the holotype, but their caudal part is damaged (Figs. 19.2–19.3). The dentary of *Bolong* is more robustly built than the elongate dentary of *Penelopognathus* (Godefroit et al., 2005), but more slender than the exceptionally deep dentary of *Fukuisaurus* (Kobayashi and Azuma, 2003). In lateral view, its ventral and dorsal borders are subparallel, and as in *Iguanodon*, *Mantellisaurus*, *Fukuisaurus*, and *Equijibus*, the rostral end of the dentary is not significantly downturned, differing from the strongly deflected dentary symphysis described in *Altirhinus* and *Protohadros*. The morphology of the rostral end of the dentary appears unique in *Bolong*. Usually in iguanodontoids, the articular surface for the predentary extends the entire height of the rostral margin of the dentary; in lateral view, the rostral end of the dentary is scoop shaped and the rostral tip of the dentary is situated at or close to the ventral margin. Conversely, in *Bolong*, the rostrodorsal articular surface for the predentary occupies less than two-thirds of the height of the dentary in lateral view, and the rostral tip is therefore situated above the ventral third of the dentary (Fig. 19.2). This peculiar morphology cannot be explained by diagenetic crushing or distortion of the rostral end of the left dentary; moreover, the left dentary is exposed in lateral view, without rotation that could influence the angle of view. The ventral and rostroventral borders of the dentary form a 140-degree angle, and below the articular surface for the predentary, the rostroventral and rostrodorsal borders form an 80-degree angle. The lateral side of the rostroventral border is depressed, marking contact with the wide and caudally directed ventral process of the predentary. The main body of the dentary is gently convex dorsoventrally along most of its length. The buccal emargination separating the tooth row from the lateral aspect of the bone increases caudally. Caudodorsally, the coronoid process is inclined slightly caudally to the long axis of the dentary. In *Jinzhousaurus*, it forms a 90-degree angle with the long axis of the bone (Barrett et al., 2009). Its apex is not rostrocaudally expanded as in more advanced hadrosauroids. The coronoid process is laterally offset with respect to the tooth row, and its apex is located slightly caudally to the last dentary tooth. As in *Iguanodon*, *Mantellisaurus*, *Ouranosaurus*, and *Jinzhousaurus*, there is no extended buccal shelf separating the coronoid process from the tooth row, thereby differing from the wide buccal shelf present in more derived hadrosauroids *Altirhinus*, *Probactrosaurus*, and *Protohadros*. The caudal part of the dentary is excavated by the large adductor fossa, which extends rostrally as a deep Meckel's groove (Fig. 19.2). Fourteen tooth positions are present. The diastema between the last tooth position and the articular surface for the predentary is not larger than two crown widths. A thin parapet, limited ventrally by a series of interconnected nutritional foramina, conceals the lingual aspect of the tooth rows (Fig. 19.2). Because the dental battery is less developed than in hadrosaurids, the parapet is also much lower.

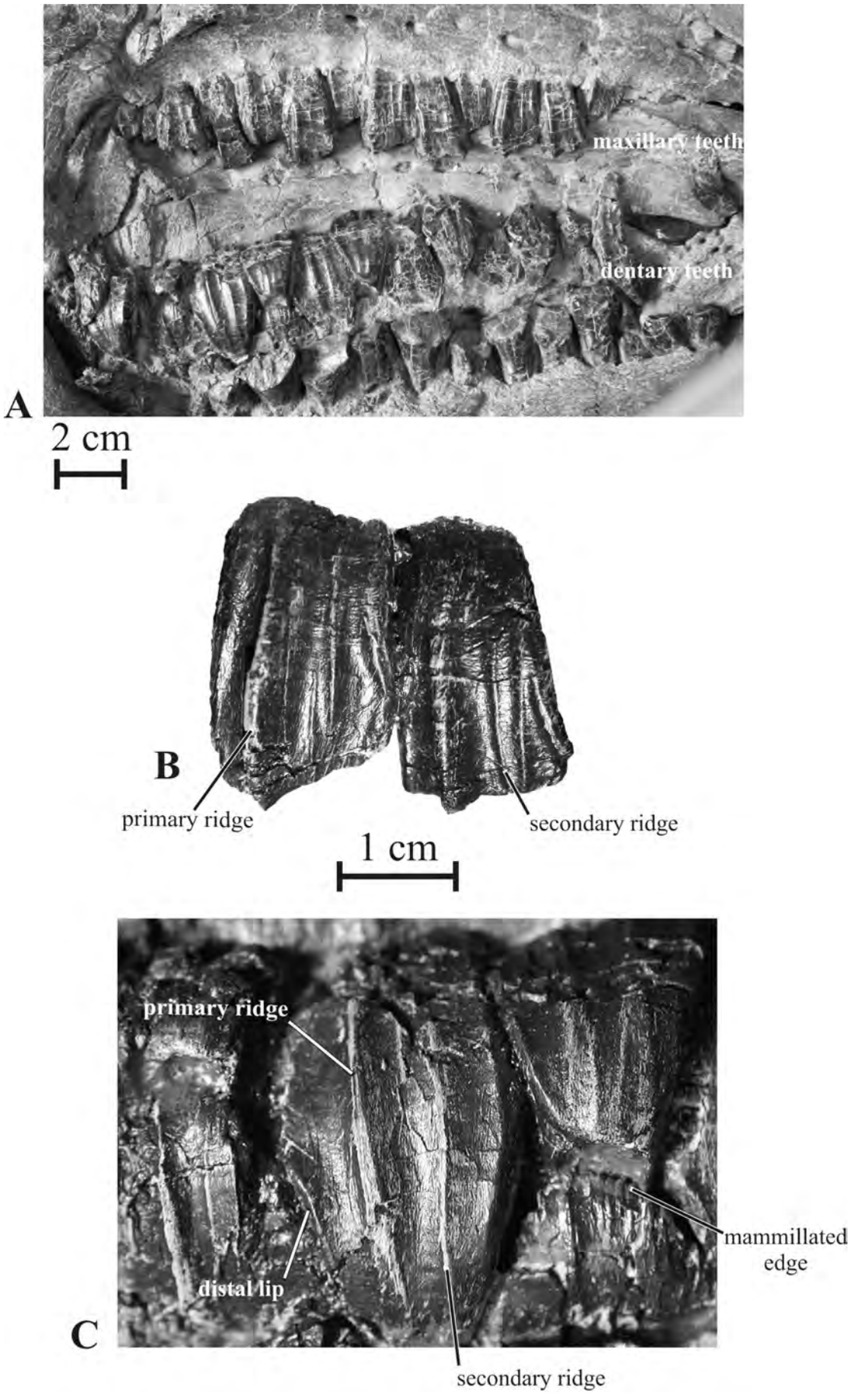

19.6. *Bolong yixianensis,* YHZ-001 (holotype). Cervical vertebrae in right lateral view. *Abbreviations:* c, cervical vertebra; n. sp., neural spine.

Surangular. Only the retroarticular process of the right surangular is preserved (Fig. 19.4). As is usual in iguanodontoids, it is lobate and upturned above the glenoid. It is mediolaterally compressed, with a thin ventral edge.

Splenial. The splenial is tentatively identified as a thin elongate plate of bone that lies against the caudomedial aspect of the dentary (Fig. 19.2). It is displaced dorsally from its natural position, across the Meckel's groove.

Prearticular. A thin rodlike element that lies dorsal to the splenial and against the caudomedial surface of the dentary is tentatively identified as the rostral portion of the prearticular (Fig. 19.2).

Teeth. The teeth of *Bolong* resemble those of *Iguanodon* and *Mantellisaurus.* There is only one functional tooth for each tooth position. Both the maxillary and the dentary teeth have long, tapering roots with shallow grooves on their mesial and distal edges to accommodate the closely packed crowns of the adjacent successional teeth. The mesial teeth are the smallest in both the maxillary and dentary tooth rows (Fig. 19.5A).

The maxillary teeth are proportionally narrower than the dentary teeth (Fig. 19.5B). The maxillary crown is lozenge shaped. An extensive dorsolaterally inclined wear facet truncates its lingual side. The labial side of the crown is thickly enameled, and the margins of the unworn partially erupted teeth are strongly denticulate. A prominent primary ridge extends along the enameled labial side of the crown. It is placed more distally than in *Iguanodon*, *Mantellisaurus*, and *Jinzhousaurus.* The primary ridge is deflected distally on all the maxillary teeth. Up to four secondary ridges are positioned mesial to the primary ridge; all extend to the apex of the crown.

The labial side of the dentary crowns is always strongly truncated because of heavy abrasion. The enameled lingual side of the crowns is asymmetrical and leaf shaped. Although the proportions of the crown are variable within the dental battery, the height/width ratio of the crown is less than 2. A primary ridge, less prominent than on the maxillary teeth, extends the entire height of the crown, dividing the crown surface into two unequal halves (Fig. 19.5C). A less prominent secondary ridge, parallel to the primary ridge, bisects the larger mesial half of the crown and always reaches the upper part of the mesial margin. One or two less clearly defined ridges extend up the lingual side of the crown mesial to the primary ridge, but they tend to merge with the surface of the crown before reaching the apex. In addition, there may be a variable number of more or less parallel subsidiary ridges, which are extensions of the bases of the marginal denticles. On the upper part of the edge of the crown, the denticulations form simple tongue-shaped structures. The structure of the marginal denticulations becomes more elaborated further down the sides of the crown. The edge becomes thickened, and each of the denticulations forms a curved and crenulated ledge, with additional mammillations, which wrap around the edge of the crown. Marginal denticulations are not developed on the edges along the lower part of the crown. At this level, the mesial edge is only slightly thickened. The distal edge forms an everted, oblique lip, as if the edge of the crown had been pinched inward. However, this distal lip is less prominent than in *Altirhinus*, *Penelopognathus*, *Batyrosaurus*, and *Probactrosaurus*, and it does not bear mammillations.

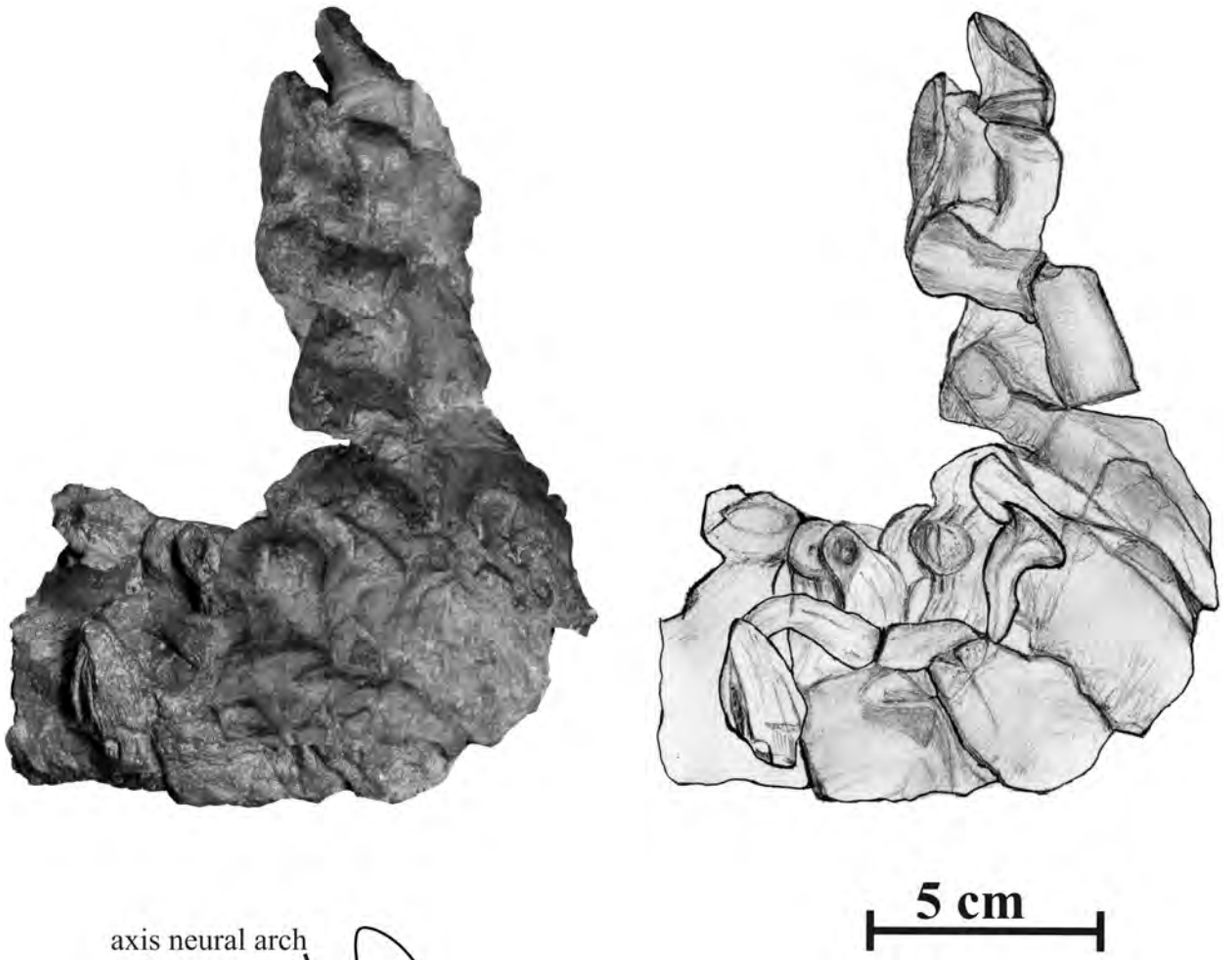

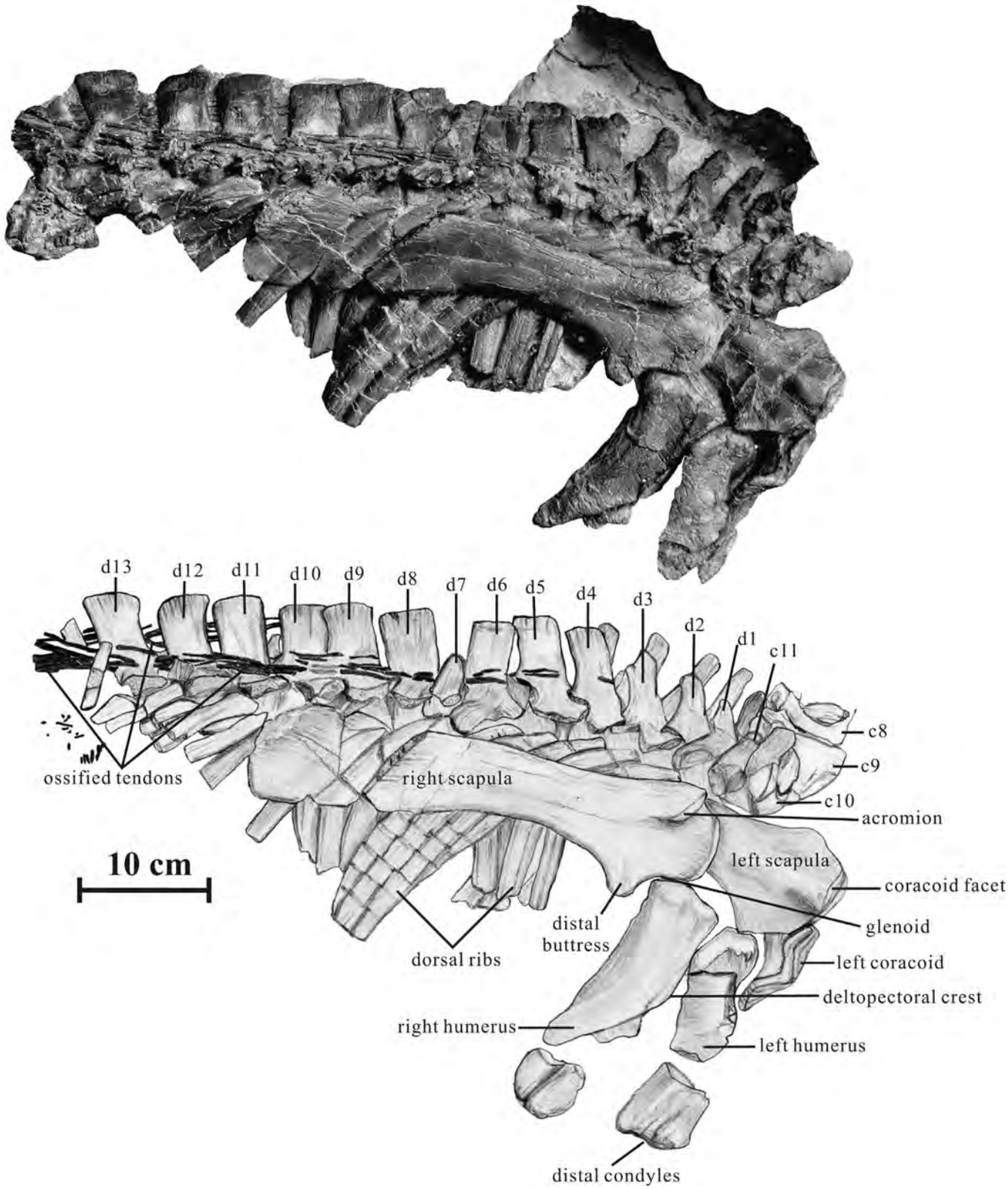

Most of the vertebral column is preserved in connection. However, the caudal part of the dorsal series and the sacrum are poorly preserved and cannot be adequately described. The distal part of the tail is missing.

Cervical vertebrae. There are 11 cervical vertebrae as in *Iguanodon*, *Mantellisaurus*, *Ouranosaurus*, and probably *Equijubus* (Figs. 19.6–19.7). The atlas neural arch is robust (Fig. 19.6). It expands cranially into robust prezygapophyseal processes. Caudally, the postzygapophyses are much smaller.

The axial centrum is poorly preserved, and its limits with the odontoid process and the axial intercentrum cannot be discerned. It appears elongated. The axial neural arch forms a large, craniocaudally expanded, neural spine. The cranioventral margin of the neural arch has an elongated prezygapophyseal process. Caudally, it forms a transverse process that projects caudolaterally and terminates in a diapophysis. Caudally, the spine bifurcates into two divergent buttresses that support the postzygapophyses.

The centra of the postaxial cervical vertebrae are opisthocoelous, with a hemispherical cranial articular surface and a deeply concave caudal surface. The centrum of the third cervical is craniocaudally elongate and longer than wide. But the centra of the succeeding cervicals appear proportionally shorter. Because of postmortem deformation and intimate articulation between adjacent opisthocoelous centra, the vertebrae cannot be adequately measured. Ventrally, the centra are transversely compressed and form a thick and rugose keel. A rounded foramen usually pierces the centrum above the keel. The parapophysis is located on the lateral side of the centrum, close to the cranial border. The neural arch is robust. Two paired processes are developed from the outer surface of the arch. The more cranially placed transverse process supports large prezygapophyses on its rostrodorsal side and also provides, at its caudal ends, the diapophyses for articulation with the cervical rib heads. The size of the transverse process regularly increases passing through the cervical series. The postzygapophyseal processes are particularly long and stout. They diverge caudally and laterally to cover the transverse process of the succeeding adjacent vertebra. The size of the postzygapophyseal processes also increases progressively along the cervical series. The neural spines of the cervical vertebrae are not preserved.

Cervical ribs. Fragments of cervical ribs are poorly preserved on the lateral aspect of the neck. All appear double-headed. A thin bony rod between the atlantal neural arch and the occipital condyle is tentatively interpreted an atlantal rib.

Dorsal vertebrae. The first 13 dorsal vertebrae are visible (Fig. 19.7). However, all the centra are completely hidden by the scapula or the dorsal ribs, and the transverse processes are eroded or destroyed. Consequently, only the neural spines can be adequately described. The neural spine of the first dorsal is slender, inclined caudally, and hook shaped. The size and the robustness of the spine increase regularly until the fifth dorsal. From this level, the spine is typically rectangular and slightly inclined caudally. The apex of the spine is slightly enlarged transversely and rugose, suggesting the presence of a cartilaginous cap in life. As in *Iguanodon*, the neural spines of the dorsals remain relatively low, contrasting with the situation observed in *Mantellisaurus*, where they are more than 2.5 times higher than

19.7. *Bolong yixianensis,* YHZ-001 (holotype). Dorsal part of the axial skeleton, pectoral girdle, and humeri in right lateral view. *Abbreviations:* c, cervical vertebra; d, dorsal vertebra;

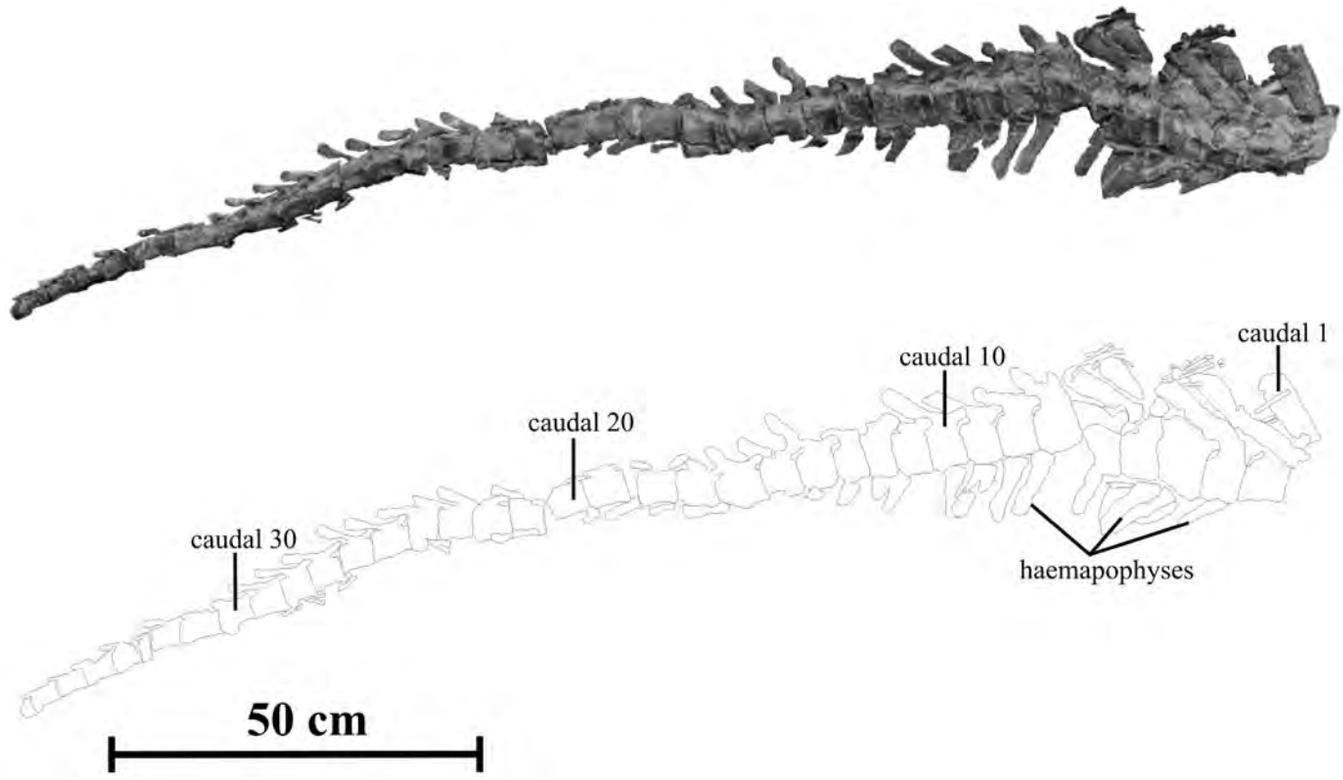

19.8. *Bolong yixianensis,* YHZ-001 (holotype). Tail in right lateral view.

the vertebral centrum and especially in *Ouranosaurus*, where the spine is as much as nine times the height of the centrum.

Dorsal ribs. Approximately 15 dorsal ribs are preserved in articulation (Fig. 19.7). However, their proximal head is hidden by the scapula and their distal portion is broken off. Therefore, nothing notable can be observed on them, except that they are curved and quite robust.

Caudal vertebrae. Thirty-seven caudal vertebrae are preserved in connection (Fig. 19.8). The centra of the proximal 15 caudals are proportionally short, higher than long, and subquadrangular in lateral view (length/height ratio = 0.82 at the level of the seventh caudal centrum). Distally, the centra become proportionally longer than high (length /height ratio = 1.86 at the level of the 36th preserved caudal centrum). The lateral sides of the centra are slightly depressed. Their ventral side is concave and forms four (two proximal and two distal) large hemapophyseal facets; the distal facets are usually better developed than the proximal ones. The dorsolateral sides of the proximal 14 centra have an elliptical and rugose articular facet for the caudal ribs. The fact that the ribs are not fused to the centrum suggests that YHZ-001 was not completely mature when it died. On the neural arch, the prezygapophyses are inclined medially, whereas the postzygapophyses are similarly inclined laterally. The neural spines of the proximal caudal vertebrae are about 1.5 as high as the centra. Although the neural spines are straight and roughly rectangular on the proximal half of the preserved portion of the tail, they become progressively curved and lobate on the distal half.

Hemapophyses. About 27 hemapophyses are preserved either articulated or not to the corresponding facets of the centra (Fig. 19.8). The first hemal arch articulates between the second and third preserved caudals.

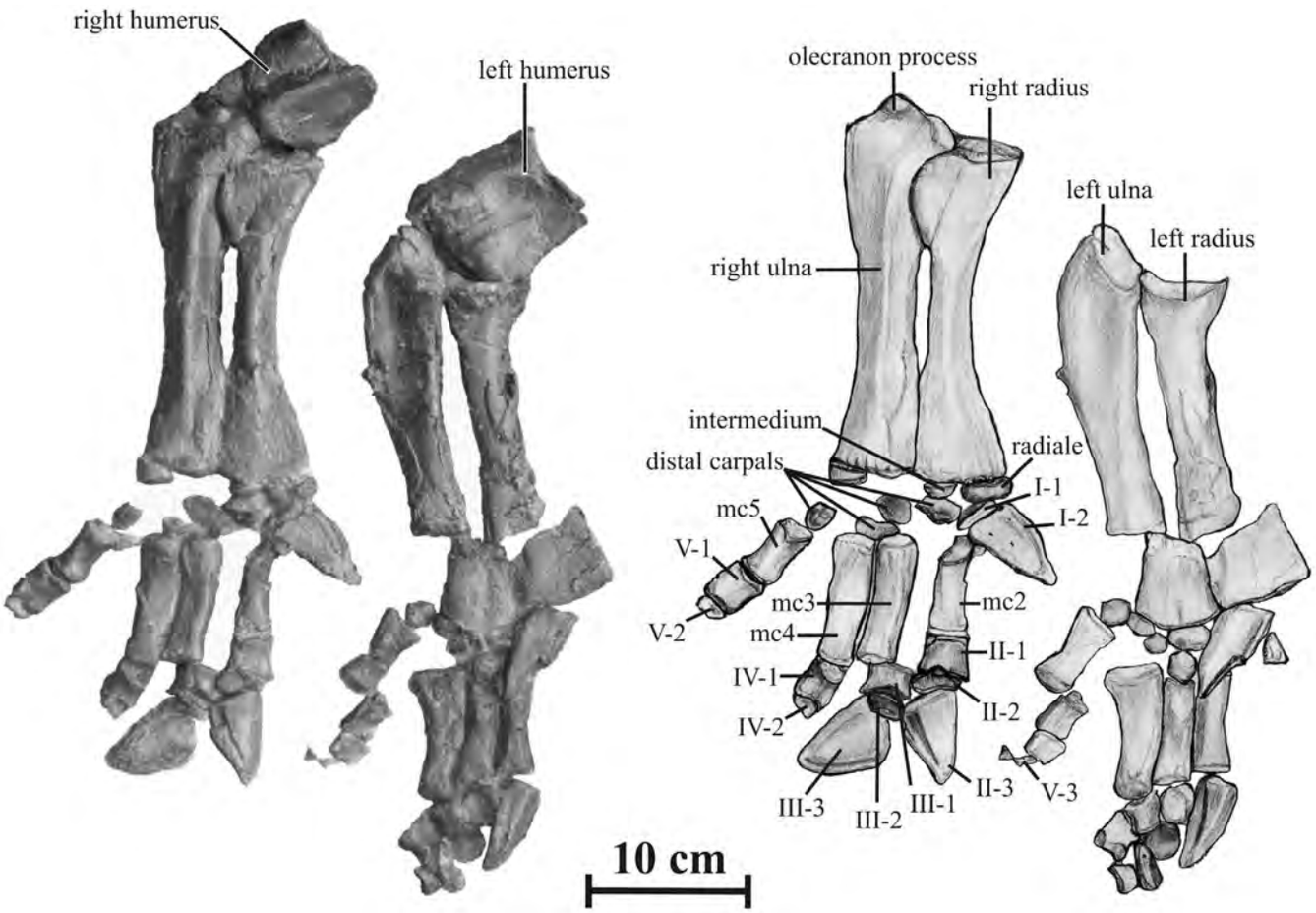

19.9. *Bolong yixianensis,* YHZ-001 (holotype). Forearms and mani in right lateral view. *Abbreviations:* mc, metacarpal; I–V, digit numbers; 1–3, phalanx numbers.

It articulates between caudal vertebrae 2–3 in *Iguanodon*, *Mantellisaurus*, and lambeosaurines (Norman, 1980, 1986), between vertebrae 3–4 in *Uranosaurus* (Taquet, 1976), distal to caudal vertebra 4 or 5 in hadrosaurines (Horner et al., 2004), and between vertebrae 7–8 in *Tethyshadros* (Dalla Vecchia, 2009). On the proximal part of the tail, the height of the chevron is roughly equivalent to the height of the corresponding neural spine; distally, it is always much lower and more slender. Their caudoventral orientation was also apparently equivalent to the caudodorsal angle of the corresponding neural spine.

Ossified epiaxial tendons. In *Bolong*, the ossified epiaxial tendons extend from dorsal 4 to about the level of the sixth preserved caudal (Fig. 19.7). Similarly, ossified tendons are to be found from dorsal 3 up to caudal 6 in the hadrosaurid *Brachylophosaurus* (Prieto-Marquez, 2007). The ossified tendons extend further distally on the tail in the basal hadrosaurid *Tethyshadros* (from dorsal 4 to caudal 20; Dalla Vecchia, 2009), in the hadrosaurine *Gryposaurus* (from dorsal 4 to caudal 19; Parks, 1920), and in the lambeosaurine *Corythosaurus* (Brown, 1916). Ossified tendons have never been reported along the cervical series in hadrosaurids (Brown, 1916). In the basal iguanodontoids *Iguanodon* and *Mantellisaurus* ossified tendons are present from cervical 10 up to about caudal 20. The arrangement of the ossified tendons appears quite primitive in *Bolong:* they are longitudinally arranged along the epaxial region of the vertebrae, between the transverse process and the base of the neural spine. On the dorsal vertebrae, they do

not extend above the proximal third of the spine. This is the plesiomorphic condition also encountered in *Hypsilophodon*, *Gasparinisaura*, *Parksosaurus*, *Thescelosaurus*, *Dryosaurus*, and *Tenontosaurus*. In *Camptosaurus*, *Iguanodon*, and *Mantellisaurus*, the epaxial tendons are arranged in a complex double-layered rhomboidal structure, and the tendons extend to the distal portion of the neural spine on the dorsal vertebrae (Norman, 1980, 1986). This is also the case in hadrosaurids, in which the epaxial tendons even form a three-layered lattice (Adams and Organ, 2005).

Scapula. The scapula is described as horizontal, as presented in Figure 19.7. The right scapula is nearly completely preserved. The proximal plate of the left one is visible in medial view. The scapula of *Bolong* is typical for basal iguanodontoids. As in, for example, *Iguanodon*, *Mantellisaurus*, *Ouranosaurus*, *Altirhinus*, and *Probactrosaurus*, the proximal plate is expanded dorsoventrally (distinctly higher than distal scapula) to support the glenoid and to provide a sutural surface for the coracoid, the acromial process is directed dorsally, and the articular facet for the coracoid is extensive. In typical hadrosaurids, the proximal plate is dorsoventrally narrow (no higher than distal scapula), the acromial process projects horizontally, and the coracoid articulation is restricted. The coracoid facet is straight and occupies much of the proximal end of the scapula, with the glenoid forming a deep embayment on the caudal corner of this surface. The glenoid is supported distally by a prominent quadrangular buttress that faces ventrally. The acromial process is thickened laterally and gradually merges with the blade. Between the coracoid suture and the acromial process, the dorsal corner of the proximal plate forms a deep notch. Distal to the proximal plate, the scapular blade has its minimal height, but it remains comparatively thick transversely. The scapular blade is slightly curved both medially (to fit against the rib cage) and ventrally. It appears proportionally better developed than in *Iguanodon*, but less curved ventrally than in *Mantellisaurus* (although it cannot be excluded that this impression results from slight postmortem deformation). It progressively becomes mediolaterally thinner distally. The dorsal and ventral borders of the scapular blade remain subparallel along most of their length; only the distal third of the blade is slightly broadened dorsoventrally.

Coracoid. The left coracoid is deformed diagenetically (Fig. 19.7). It roughly resembles that of the basal iguanodontoids *Iguanodon*, *Mantellisaurus*, *Ouranosaurus*, and *Probactrosaurus:* it is large (coracoid/scapula lengths >0.2), and the articular surface for the scapula is longer than the glenoid. In hadrosaurids, the coracoid is proportionally shorter (coracoid/scapula lengths

Ulna. The ulna is notable for being proportionally short but particularly robust in *Bolong* (Fig. 19.9), with ratio of craniocaudal height of proximal part/length = 0.28. The olecranon process of the ulna is prominent, blunt, and rounded. The humerus articulated against its convex cranial surface. The medial and lateral proximal processes are also particularly high and robust, and the articular facet for the proximal part of the radius is correspondingly deep. The caudal border of the proximal ulna forms a prominent keel. The ulna progressively tapers but is craniocaudally expanded distally.

Radius. With ratio of craniocaudal height of proximal part/length = 0.28, the radius is also robust. The proximal and distal ends of the ulna

are nearly symmetrically expanded craniocaudally and are triangular in mediolateral view (Fig. 19.9). Between the proximal and distal expansions, the shaft of the radius is circular in cross section. Because of the craniocaudal expansions of the extremities of these bones, a gap is present between the radius and the ulna, probably allowing for some ability for pronation/supination of the antebrachium.

Carpus. Six carpal elements are preserved in the right manus (Fig. 19.9). However, it is difficult to identify them precisely because they have been displaced. Some elements can also be observed in the left wrist, but they are too poorly preserved to be adequately described. The carpals remain separate elements in *Bolong*, and contrary to *Iguanodon*, *Mantellisaurus*, and *Ouranosaurus*, they do not co-ossify into two blocks. The ulnare is not preserved. The radiale is a mediolaterally elongated element that closely fits the cranial part of the distal surface of the radius. Its convex distal surface articulates with the flattened first phalanx of digit I. It is possible that metacarpal I is completely fused to the radiale, as observed in *Camptosaurus* (Erickson, 1988), although this cannot be conclusively demonstrated. The intermedium is tentatively interpreted as a small, flattened element that fits against the caudal portion of the articular surface of the radius. Distal carpals 2–5 form flattened and convexoconcave bones close to the proximal end of the corresponding metacarpals.

The hand of *Bolong* shows functional similarities with that of *Iguanodon*, *Mantellisaurus*, and *Ouranosaurus*. The first digit has an enlarged, probably divergent, spinelike ungual, the middle three digits form a rather compact unit that presumably allows for some degree of hyperextension, and the fifth digit was apparently long, flexible, and opposable (Norman, 1980, 1986).

Metacarpals. The metacarpals are proportionally much shorter and more robust than in *Iguanodon*, *Mantellisaurus*, and *Ouranosaurus* (Fig. 19.9).

Metacarpal II is moderately well preserved on both hands. It is more slender than metacarpals III and IV and somewhat transversely compressed. Its medial side is regularly convex, whereas its lateral side is slightly concave where it was closely bound to metacarpal III. The distal articular surface is slightly expanded mediolaterally and forms a shallow intercondylar groove.

Metacarpal III is longer and more robust than metacarpal II. Its shaft is quadrangular, with a flattened dorsal side. In craniocaudal view, its medial side is slightly sigmoidal where it closely articulates with metacarpal II. The proximal articular surface is not expanded and weakly convex. The distal articular surface is slightly expanded mediolaterally, with a shallow intercondylar groove.

Metacarpal IV is as long as metacarpal III but appears more robust because of the development, at midheight on its dorsal side, of a medial lip that partially covered metacarpal III, reinforcing the attachment between these metacarpals. The proximal articular surface is well expanded and mediolaterally convex. The distal articular surface is more reduced than the proximal one and convex; there is no trace of an intercondylar groove.

Metacarpal V is the shortest of the series. Its proximal articular surface is mediolaterally expanded and shallowly concave. The distal articular surface is only slightly expanded, broadly convex, and devoid of an intercondylar

groove. Between the articular surfaces, the shaft of metacarpal V is strongly constricted.

Manus digits. If the first three digits of the right manus of YHZ-001 are complete, distal phalanges may be missing on digits IV and V (Fig. 19.9). The fifth digit of the left hand is apparently complete. From what can be observed in the holotype, the phalangeal formula of the manus of *Bolong* is 2–3–3–(2+)–4. It is 2–3–3–2–4 in *Iguanodon* and 2–3–3–3–3 in *Mantellisaurus.* In general, the proximal and intermediate phalanges in the manus of *Bolong* are proportionally much shorter than in *Iguanodon*, *Mantellisaurus*, *Ouranosaurus*, *Altirhinus*, and *Probactrosaurus*.

The first phalanx of digit I is a thin, mediolaterally elongated oval disc between the radiale and the large ungual phalanx. The ungual phalanx is quite characteristic for basal iguanodontoids: it is straight, triangular, and mediolaterally compressed, as in *Altirhinus.* Ungual grooves are well developed on either side of the dorsal surface and are supported by a prominent shelf. In *Iguanodon*, *Mantellisaurus*, and *Ouranosaurus*, the pollex is more conical and spikelike.

Digit II is formed by three phalanges. The first phalanx is short and trapezoidal in dorsal view, contrasting with the elongated and slender first phalanx in the second digit of *Mantellisaurus* and *Altirhinus.* Both the proximal and distal articular surfaces are dorsoventrally concave and extend onto the dorsal surface of the phalanx, suggesting that the second digit could be hyperextended. The second phalanx is a short, wider than long, blocklike element. It is roughly triangular in dorsal view. Its proximal articular surface is oblique and extends onto the ventral surface of the phalanx. Its distal articular surface is dorsoventrally convex. The ungual is nearly as large as that of the first digit, triangular in dorsal view, and dorsoventrally flattened. The ungual grooves are deep on either side of the dorsal surface, limiting a triangular central surface.

The third digit comprises three phalanges. The first and second phalanges have the same morphology as the corresponding phalanges of digit II but are proportionally shorter. The orientation of the articular surfaces shows that this digit could also be hyperextended. The ungual appears slightly more massive than in digit II and terminates in a bluntly rounded point. However, it is proximodistally longer than mediolaterally wide, contrasting with the condition seen in *Iguanodon* and *Mantellisaurus*, in which the ungual of digit III is hooflike and as wide as long.

Only the proximal phalanx of digit IV is preserved in both mani. A small fragment of the second phalanx can be observed on the right hand. The first phalanx is trapezoidal in dorsal view. Its dorsal side is regularly convex mediolaterally. It is asymmetrical in dorsal view. The proximal articular surface is shallowly concave and extends onto the dorsal side of the phalanx. The distal articular surface is dorsoventrally convex and also invades the dorsal side of the phalanx; it forms a well-developed intercondylar groove. This morphology suggests that digit IV could also be hyperextended. The proximoventral surface forms well-developed condyles marked by rugosities, which probably represent the scars of some ligaments that helped to bind the adjacent phalanges.

Digit V has four phalanges, as in *Iguanodon*. The first phalanx is robust and quadrangular in dorsal view. Its dorsal surface is shallowly

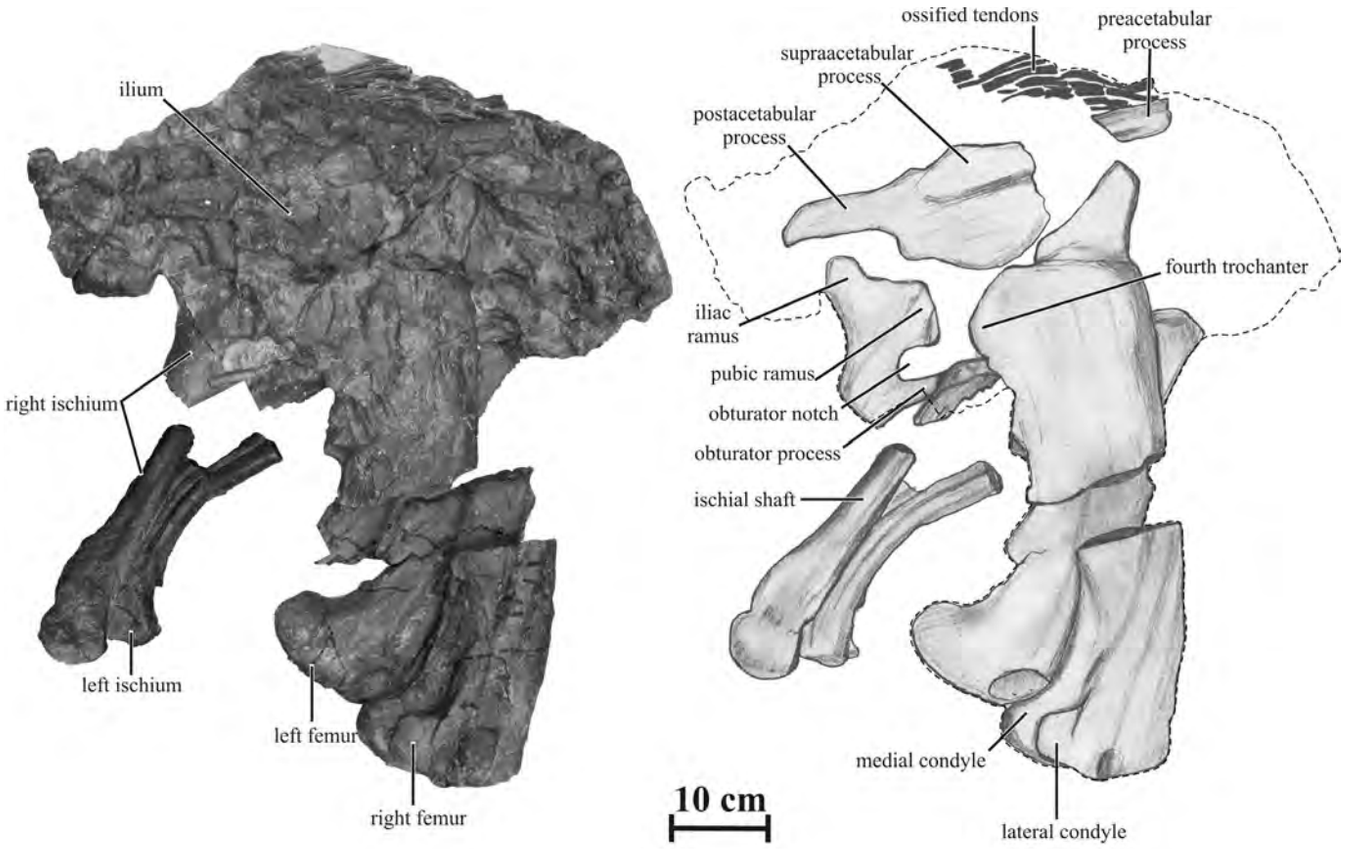

19.10. *Bolong yixianensis,* YHZ-001 (holotype). Sacral part of the axial skeleton, pelvic girdle, and femora in right lateral view. The dashed lines indicate the limits of the block.

concave. Its proximal articular surface is only slightly expanded mediolaterally and shallowly concave. Its distal articular surface is slightly convex dorsoventrally; it forms a shallow intercondylar groove. The second phalanx is much eroded and cannot be adequately described. It is about half the length of the first phalanx and trapezoidal in dorsal view. The third phalanx is poorly preserved and appears subtriangular in dorsal view. The fourth phalanx is a tiny triangular element that forms a shallowly convex proximal articular surface and bears a strong median ridge on its dorsal side.

Ilium. The right ilium is crushed (Fig. 19.10). The postacetabular process is remarkably narrow dorsoventrally (ratio length/maximal height [taken at the level of its cranial end] = 2). This ratio is >2 in *Tethyshadros* and in some hadrosaurines (e.g., *Gryposaurus*, *Edmontosaurus*, and *Anatotitan*) as a result of elongation of the postacetabular process of these taxa (Dalla Vecchia, 2009, fig. 5B). The dorsal edge of the postabular process is straight; however, the postacetabular notch is much deeper than in *Iguanodon*, *Mantellisaurus*, *Ouranosaurus*, *Altirhinus*, *Bactrosaurus*, and *Tethyshadros*. The main body of the ilium is about two times higher than the postacetabular process. Although it is crushed, its dorsal margin is convex in lateral view, without a distinct depression over the supracetabular process as is usually observed in hadrosaurids. The supracetabular process is poorly developed. The ventral part of the ilium (including the ischiac and pubic peduncles) is destroyed. The preacetabular process is also incompletely preserved. It is robust and weakly deflected ventrally, with a thick dorsal border.

Ischium. The proximal end of the ischium is dorsoventrally expanded, transversely flattened, and triradiate, formed by an iliac ramus, a pubic ramus, and an obturator process (Fig. 19.10). The iliac ramus is the largest. Its dorsal end is thickened laterally and rugose, and it abuts the ischial peduncle of the ilium. The pubic ramus is also transversely compressed and hatchet shaped. A large triangular oburator process is present on the ventral side of the proximal portion of the ischial shaft. The salient and thin caudoventral corner of the pubic ramus and the obturator process enclose a deep obturator notch. The semicircular shape of this notch closely resembles the condition that can be observed in *Altirhinus*, *Probactrosaurus*, *Bactrosaurus*, and Hadrosauridae. In *Iguanodon* and *Tethyshadros*, the obturator process is located more distally on the ventral side of the ischial shaft and the obturator notch is proportionally wider and less deep. Although it is incompletely preserved, the ischial shaft is robust, transversely compressed, and straight. It terminates distally as a moderately expanded knob.

Femur. The right femur is crushed against the left one and is consequently completely deformed. Moreover, its proximal half is largely destroyed, and a 7-cm portion of its shaft is missing (probably lost during excavation; Fig. 19.10). The femur of *Bolong* appears proportionally short and wide (although it may be an artifact of deformation) and is slightly recurved in lateral view (unlike the straight form seen in hadrosaurids). Above the midheight of the shaft, a prominent triangular fourth trochanter projects from the caudomedial edge. The distal portion of the shaft is bowed cranially and the distal condyles are prominently expanded, mainly caudally. The medial condyle appears larger and more robust than the lateral one. The lateral side of the lateral condyle bears a prominent rounded vertical ridge that separates the flattened caudal heel region from the more cranial lateral surface of the condyle. The flexor intercondylar groove extends proximally along the caudal side of the femoral shaft as a deep furrow. The extensor intercondylar groove is not visible.

Tibia. The left tibia can be observed in medial view and the right one in cranial view (Fig. 19.11). Compared with other basal hadrosauroids, the tibia of *Bolong* is proportionally short and robust. Its proximal end is craniocaudally enlarged. The cnemial crest is weakly developed. It is oriented laterally and supported by a rounded ridge down the cranial side of the proximal third of the tibial shaft. The caudal corner of the medial side of the tibia forms a large internal proximal condyle. The deformed cnemial crest of the right tibia hides the lateral proximal condyles. In medial view, the caudal margin of the tibia is regularly concave. The distal half of the tibia is craniocaudally constricted, whereas its distal third expands transversely. The external malleolus is prominent distally. Its craniodistal surface articulates both with the calcaneum and the astragalus. Above the external malleolus, the lateral side of the distal tibia has a deep, triangular, and rugose area, marking the contact with the distal fibula. The internal malleolus is more prominent than the external malleolus and its distal surface articulates with the astragalus. Above the distal malleoli is a deep triangular depression on the distal third of the cranial side of the tibia.

Fibula. The right fibula of YHZ-001 is visible in lateral view (Fig. 19.11). It is more robustly built than in *Mantellisaurus* and *Probactrosaurus*. Proximally, the fibula is craniolaterally expanded and transversely compressed.

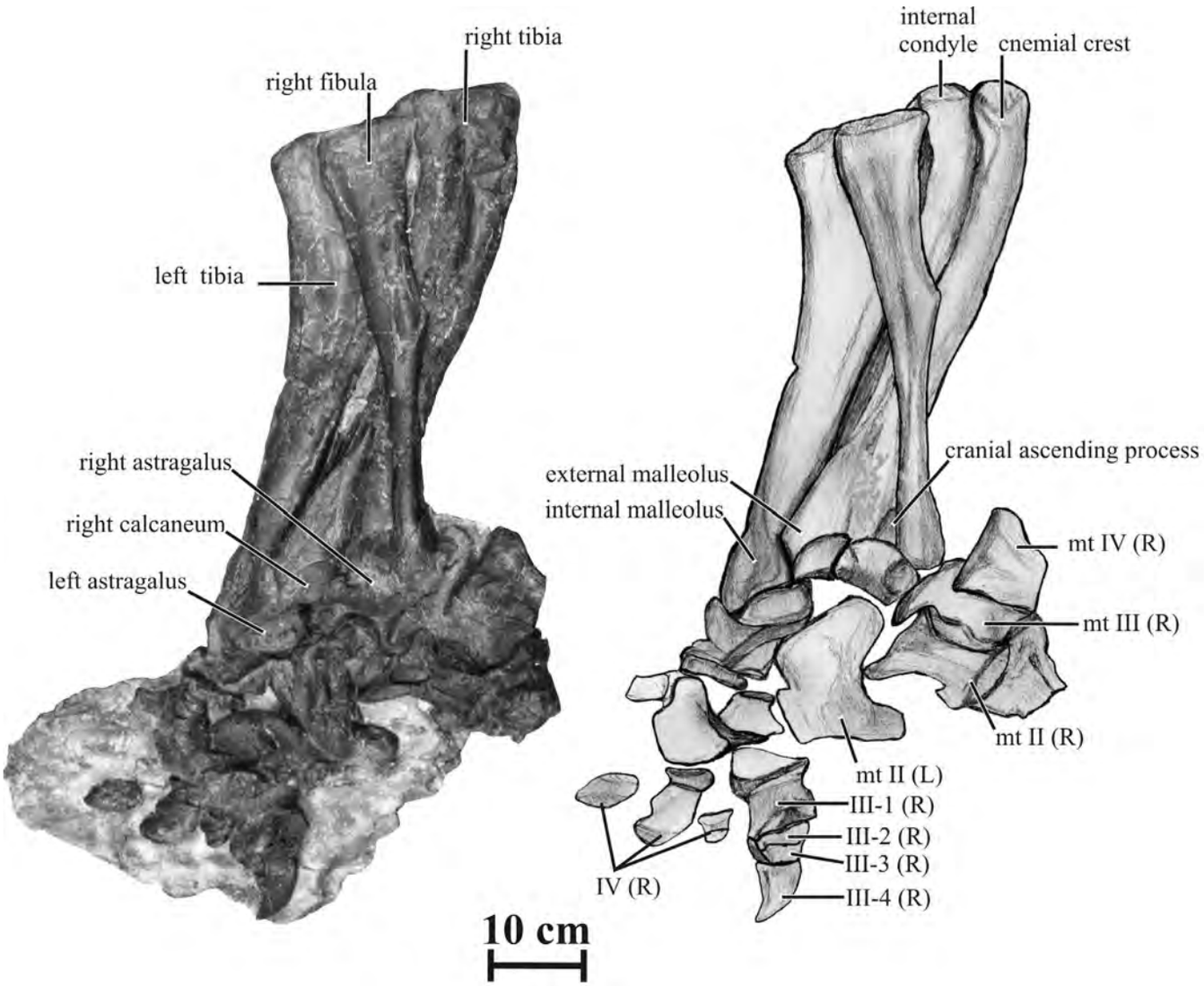

19.11. *Bolong yixianensis,* YHZ-001 (holotype). Tibiae, right fibula, and pes. *Abbreviations:* L, left; R, right.

The fibular shaft progressively narrows distally, and its distal end forms a moderately developed and slightly everted bootlike structure, which articulated against the craniolateral edge of the distal end of the tibia.

Astragalus. The right astragalus, closely appressed to the distal articular surface of the tibia, is visible in cranial and distal views. The left one is visible only in medial view (Fig. 19.11). It contacts the calcaneum laterally, but these two bones remain unfused. Its distal articular surface is regularly convex in mediolateral view, concave in craniocaudal view, and rugose. The triangular cranial ascending process, which lies against the cranial side of internal distal malleolus of the tibia, is high compared to the low ascending process seen in *Mantellisaurus* (Norman, 1986, fig. 59B). In cranial view, it is subtriangular and distinctly skewed medially.

Calcaneum. The right calcaneum is visible in cranial view and partly in distal view (Fig. 19.11). It is closely appressed to the external distal malleolus of the tibia and to the astragalus. Its distal articular surface is rugose and convex in mediolateral view. The craniomedial corner of the calcaneum forms a high, triangular, and medially skewed ascending process, which lies against the cranial side of the external distal malleolus of the

tibia. This process is unusual in iguanodontoids but has been described in *Bactrosaurus* (Godefroit et al., 1998).

Metatarsals. Few elements of the left foot (including metatarsal II) of the left foot can be observed in medial view. The right foot is more complete, but most bones are eroded and disarticulated, making identification difficult (Fig. 19.11). The metatarsals are proportionally shorter and more robust than in other basal iguanodontoids where it can be observed; ratio metatarsal III/femur = 0.18 in *Bolong*, 0.39 in *Iguanodon* (Norman, 1980), 0.37–0.39 in *Mantellisaurus* (Norman, 1986), 0.37 in *Ouranosaurus* (Taquet, 1976), 0.37 in *Probactrosaurus* (P.G., pers. obs.), 0.36 in *Tenontosaurus* (Winkler et al., 1997), 0.37 in *Nanyangosaurus* (Xu et al., 2000), 0.35 in *Tethyshadros* (Dalla Vecchia, 2009), 0.37–0.41 in *Edmontosaurus* (Lull and Wright, 1942), and 0.37–0.41 in *Corythosaurus* (Lull and Wright, 1942).

Metatarsal II is mediolaterally compressed. Its proximal articular end is expanded dorsoventrally. Proximomedially, a large concave surface closely abuts the shaft of metatarsal III. The shaft of metatarsal II is strongly constricted dorsoventrally. Its dorsal side is more concave than its ventral side. In distal view, its distal end expands to form a large saddle-shaped articular surface for the first phalanx.

Metatarsal III is poorly preserved. Proximally, its lateral side forms a wide, deep, and triangular depression for tight articulation with metacarpal IV.

Metatarsal IV is also incomplete and poorly preserved. It appears much more slender than metatarsal III, and its distal end is only slightly expanded dorsoventrally and smoothly convex.

Pedal phalanges. Only the distal end of phalanx II-1 is preserved in connection with metatarsal II (Fig. 19.11). No other phalanges were identified from digit II.

Digit III has four phalanges, as is usual in Iguanodontia. The first phalanx is robust and mediolaterally wider than proximodistally long, contrasting with the more elongated first phalanx in *Mantellisaurus* and *Probactrosaurus*. The short shaft is mediolaterally constricted between the proximal and distal articular surfaces. The distal articular surface is broad and convex, with a shallow intercondylar groove, and the surface extends on the dorsal (extensor) side of the phalanx. The second and third phalanges are short disklike elements. The ungual phalanx is robust and arrowhead shaped in dorsal view. It is not as proximodistally shortened and genuinely hoof shaped as in the majority of hadrosaurids. From its wide and thick proximal end, it becomes dorsoventrally flattened toward its tip, and its distal end is strongly arched ventrally. The distal end is eroded, but it was apparently less blunt than in *Iguanodon* and *Mantellisaurus*. The claw grooves are better developed than in *Probactrosaurus* and are supported by a shelf.

Several phalanges are visible in digit IV (the ungual is not preserved). However, their state of preservation is poor, and they cannot be formally identified. They are much smaller (about half the size) than the phalanges of digit III.

Although histological analyses have not been carried out, the complete closure of the sutures between the neural arches and centra throughout the vertebral column is suggestive of skeletal maturity in the holotype specimen of *Bolong*. However, the caudal ribs are not fused to the centra, indicating that sexual maturity was probably not completely achieved. As discussed above, we estimate a body length of 3 m for this individual, which is particularly small by the standard of known basal iguanodontoids. *Jinzhousaurus*, also from the middle part of the Yixian Formation, is distinctly larger, reaching a maximal length of about 5–5.5 m (R. Pan, pers. comm.). *Bolong* has about the same size as the dwarf basal Iguanodontia *Zalmoxes robustus*, from the Maastrichtian of Romania (Weishampel et al., 2003).

It is well known that the Jehol Biota dinosaur fauna is dominated by small-bodied taxa (<3m in body length; see above). Barrett and Wang (2007) proposed two hypotheses to account for this skewed body size distribution: (1) genuine scarcity of large taxa, perhaps due to resource limitations or local physical conditions that created habitats inappropriate for large animals; and (2) presence of a taphonomic bias that precluded the preservation of large taxa. Resource limitation and climatic constraints are unlikely because of the extraordinary diversity of the fauna. The great abundance of fossil tree trunks in different localities indicates that part of this area was covered by forest, limiting the movements of larger dinosaurs. However, many different ecosystems are probably represented in the Jehol Biota. Additional work is required to determine paleoenvironmental conditions during Jehol times in order to examine how these may have influenced the composition and evolution of this biota (Barrett et al., 2009).

Assessment of the relative proportions of fore- and hind limbs in *Bolong* is complicated by the poor preservation of the humeri and femora, preventing accurate measurements. The forelimb appears proportionally much shorter than in typical quadrupedal dinosaurs and in *Iguanodon bernissartensis* (humerus is 77–80% of femoral length; Norman, 1980) and more closely resembles the condition encountered in *Mantellisaurus atherfieldensis* (humerus is 58–56% of femoral length). However, the distal portion of the forelimb is particularly short in *Bolong*, similar to vertebrates that use their forelimbs to support weight (Norman, 1980). The absence of coossified carpals suggests that the hand was, in any case, less well adapted for supporting weight that that of *Iguanodon* and *Mantellisaurus*. It may be tentatively hypothesized that Bolong spent considerable periods of time walking or running bipedally, but it may have been a facultative quadruped, as in many other nonhadrosaurid iguanodontians (Norman, 2004).

However, the proportionally short metatarsals suggest that *Bolong* was a quadrupedal dinosaur. Indeed, Galton (1970) showed that graviportal mammals and typical quadrupedal dinosaurs are characterized by a low metatarsal III/femur ratio (respectively, 0.10–0.26 and 0.12–0.26). Although the femur cannot be adequately measured in *Bolong*, the metatarsal III/tibia ratio is 0.18, indicating that the metatarsal III/femur ratio probably fell within the range of ratios found in quadrupedal dinosaurs and graviportal mammals. Therofore, the posture and gait of *Bolong* remain problematic

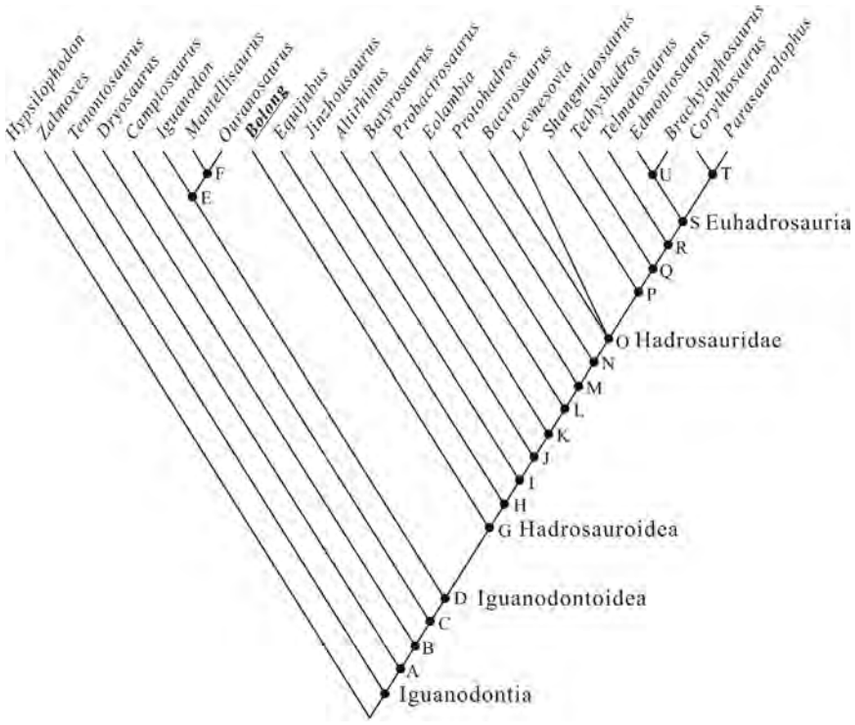

19.12. Strict consensus tree of Iguanodontia, showing the phylogenetic relationships of *Bolong yixianensis*. Letters correspond to nodes defined in Appendix 19.4.

Phylogenetic Relationships of *Bolong*

We undertook a numerical cladistic analysis of Iguanodontia to resolve the phylogenetic position of *Bolong*. According to Norman (2004), Iguanodontia is a stem-based taxon defined as all euornithopods closer to *Edmontosaurus* than to *Thescelosaurus*. This analysis is based on 25 terminal species whose skeletal remains are well preserved and/or well documented in the literature. *Hypsilophodon* was chosen as outgroup because it is known by abundant material and particularly adequately described. Other taxa (among them *Rhabdodon*, *Planicoxa*, *Valdosaurus*, *Draconyx*, *Lurdusaurus*, *Fukuisaurus*, *Muttaburasaurus*, *"Probactrosaurus" mazongshanensis*, *Penelopognathus*, and *Nanyangosaurus*) were initially included, but they were subsequently removed because of their paucity of character information, which considerably reduced the phylogenetic robustness of the analysis or obscured the general structure of the consensus tree. In this analysis, Iguanodontia are treated at the generic level, although several taxa genera are widely considered to contain more than one species. As a general rule, the type species was chosen as reference for multispecific genera. This analysis is based on 108 cranial, dental, and postcranial characters (character list in Appendix 19.2 and data matrix in Appendix 19.3), mainly compiled from the literature (Norman, 2002, 2004; Weishampel et al., 2003; You et al., 2003a, 2003b; Horner et al. 2004; Godefroit et al., 2004, 2008; Evans and Reisz, 2007; Butler et al., 2008; Sues and Averianov, 2009). Postcranial characters of *Jinzhousaurus* were not included in this analysis because the description of the postcranium of this iguanodontoid (Wang et al., 2011) was published after the present analysis was completed. The 108 characters were equally weighted and analyzed by PAUP*4.0b10 software (Swofford, 2000), both with accelerated (ACCTRAN) and delayed (DELTRAN) transformations. To assess the repeatability of tree topology, a bootstrap analysis was performed (1,000 replicates using the heuristic algorithm in PAUP). Three equally

parsimonious trees of 185 steps resulted from a heuristic search, with a consistency index of 0.72, a retention index of 0.90, and a rescaled consistency index of 0.65. The strict consensus tree is presented in Fig. 19.12 and the tree description in Appendix 19.4.

According to the present phylogenetic analysis, Iguanodontoidea form a particularly robust robust (bs = 97%) clade, characterised by the following unambiguous synapomorphies (that diagnose a clade under both ACCTRAN and DELTRAN optimizations): the supraoccipital is excluded from the dorsal margin of the foramen magnum by the paired exoccipitals (character 24); the dorsal process of the maxilla is caudal to center (character 29); the maxilla and jugal form a "finger-in-recess" suture (character 32); 18–30 tooth positions are present in the dentary tooth row (character 55); the marginal denticles along the tooth crowns are developed as curved, mammillated ledges (character 62); the sternal is hatchet shaped (character 82); the unguals on manual digits II and III are flattened, twisted, and hooflike (character 90); digit V is elongated, with three or four phalanges (character 91); the caudal ramus of the pubis is shorter than the ischium and there is no pubic symphysis (character 99): the prepubic process is expanded distally (character 101); the fourth trochanter of the femur is tab shaped (character 103); pedal digit I is absent (with the exception of metatarsal I; character 106); and pedal unguals are hoof shaped, but not broader than long, with prominent claw grooves retained (character 108).

According to our phylogenetic analysis, Iguanodontoidea can be subdivided into two clades: Iguanodontidae and Hadrosauroidea. Contrary to other recent phylogenetic analyses (e.g., Head, 1998; Norman, 2002, 2004; Sues and Averianov, 2009), we retain a monophyletic Iguanodontidae, including *Iguanodon*, *Mantellisaurus*, and *Ouranosaurus*. This clade is characterized by the following autapomorphies: the ossified epaxial tendons extend cranially from cervical 10 (character 76; the polarity of this character cannot be observed in *Ouranosaurus*) and the pollex is spikelike and conical (character 89, 0 to 2). Within Iguanodontoidae, *Mantellisaurus* and *Ouranosaurus* are united by the presence of elongated neural spines on the posterior dorsals and sacrals, which are more than 2.5 times the centrum height (character 73). The low bootstrap value (bs = 53%) clearly indicates that the relationships within Iguanodontidae remain highly conjectural in the current state of our knowledge. Moreover, newly named iguanodontid genera (see Chapter 15 in this book) need to be tentatively included in this phylogenetic analysis.

Hadrosauroidea is defined as all Iguanontoidea closer to *Parasaurolophus* than to *Iguanodon* (Sereno, 1997, amended). In our analysis, this clade is characterized by the following unambiguous synapomorphies: the antorbital fenestra is not open on the lateral side of the skull (character 26); the basipterygoid process extend ventrally well below the level of the ventral border of the occipital condyles (character 42, 1 to 0); the carpals are well ossified but remain unfused (character 86, 1 to 0); the ischium is nearly straight in lateral view (character 96, 1 to 0). *Bolong* is here regarded as the most basal Hadrosauroidea. Indeed, the antorbital fenestra is still present as a small depression between the lacrimal and maxilla, although it is not exposed laterally in other hadrosauroids (character 26, 1 to 2), and the tooth roots are not cemented at all, contrary to more advanced hadrosauroids

(character 61). *Jinzhousaurus*, also from the Yixian Formation of western Liaoning province, shares an additional dental synapomorphy with more advanced hadrosauroids: the maxillary teeth bear a single faint accessory ridge (character 65). Thus, *Bolong* apparently occupies a more basal position in the phylogeny of hadrosauroids than *Jinzhousaurus*. The phylogeny of more advanced Hadrosauroidea is discussed in Chapter 20 of this book.

Paleogeography of Basal Iguanodontia and Iguanodontoidea

The oldest Iguanodontia is *Callovosaurus leedsi*, which is based on an isolated femur from the Callovian of England (Ruiz-Omeñaca et al., 2007). During the Kimmeridgian, Iguanodontia had a Neopangean (Pangea without China and Siberia; Russell, 1993) distribution: diagnosable iguanodontians have been discovered in North America (*Dryosaurus altus*, *Camptosaurus dispar*), Europe (*Camptosaurus prestwichii*), and Africa (*Dryosaurus lettowvorbecki*). Isolated femora were also discovered in the Kimmeridgian–Tithonian of Portugal (Galton, 1980). Iguanodontia are apparently absent from Late Jurassic localities in Asia. During the Lower Cretaceous, Iguanodontia achieved a virtually cosmopolitan distribution (Norman, 2004). Basal Iguanodontia and Iguanodonidae apparently kept a Neopangean distribution, in Europe (*Iguanodon*, *Mantellisaurus*, and taxa recently named from England; see Norman, Chapter 15 in this book), Africa (*Ouranosaurus*, *Lurdusaurus*), North America (*Tenontosaurus*, "*Iguanodon*" *ottingeri*, *Dakotadon*, *Planicoxa*, *Cedrorestes*, and forms to be described from Cedar Mountain Formation in Utah; McDonald et al., 2009), Australia (*Muttaburasaurus*), and possibly South America (the phylogenetic position of *Talenkauen* and *Macrogryphosaurus*, regarded as Iguanodontia by Calvo et al., 2007, is still problematic according to Butler et al., 2008). Norman (1996) tentatively identified fragmentary remains ("*Iguanodon orientalis*") from the Lower Cretaceous of Mongolia as *I. bernissartensis*, but these fossils could just as well belong to some basal hadrosauroid; the maxillary teeth more closely resemble those of *Altirhinus*, for example, than those of *Iguanodon*.

Although basal Iguanodontia and Iguanodontidae are not confidently represented in Lower Cretaceous deposits from Asia, Hadrosauroidea have clearly an Asian origin. Indeed, Figure 19.12 shows that the most basal Hadrosauroidea (successively *Bolong*, *Equijubus*, *Jinzhousaurus*, *Altirhinus*, *Batyrosaurus*, and *Probactrosaurus*) are all from Asia. "*Probactrosaurus*" *mazongshanensis*, *Fukuisaurus*, *Nanyangosaurus*, *Penelopognathus*, and *Jintasaurus* have not been included in the phylogenetic analysis, but they are also potential basal Hadrosauroidea from the Lower Cretaceous of Asia. According to Russell (1993), the isolation of Central Asia came to an end during the Aptian–Albian, when a land route opened across the Bering Strait, although another intermittently emergent route appeared at about the same time toward Europe (Doré, 1991). The presence of the iguanodontoids *Bolong* and *Jinzhousaurus* in the middle part of the Yixian Formation indicates that connections between Asia and North America and/or Europe were already established during the lower Aptian or even during the upper Barremian. Information on the paleogeography of basal Ornithomimosauria (see Chapter 26 in this book) also suggests dinosaur immigrations from Europe into Asia during or before the Barremian. The

oldest nonhadrosaurid Hadrosauroidea outside Asia is *Eolambia*, from the latest Albian (Garrison et al., 2007) Mussentuchit Member of the Cedar Mountain Formation in Utah that includes other taxa with Asian affinities, such as tyrannosauroids, ceratopsians, and pachycephalosaurs. These records are the earliest known representatives of these groups in western North America (Cifelli et al., 1997; McDonald et al., 2010). These occurrences can be attributed to an immigration of Asian taxa, including Hadrosauroidea, into western America following the establishment of the Bering land bridge in the Aptian–Albian (Russell, 1993). The paleogeography of more derived Hadrosauroidea is discussed in Chapter 20 of this book.

Although Hadrosauridae were the most abundant and diversified large vertebrates in Laurasia during the closing stages of the Late Cretaceous (Horner et al., 2004), basal Iguanodontia (*Rhabdodon*, *Zalmoxes*) subsisted in Europe during the Campanian and the Maastrichtian (see Chapters 31 and 31 in this book), implying a long ghost lineage duration for this small clade (Weishampel et al., 2003).

Appendix 19.1. Measurements

L, left; R, right.

Preorbital length: 284 mm
External naris (L): length: 129 mm
External naris (L): maximum height: 39 mm
Maxilla (L): length: 211 mm
Maxilla (L): maximum height: 66 mm
Quadrate (R): height: 200 mm
Dentay (L): length (from rostral tip to apex of coronoid process): 275 mm
Dentary (L): height (at midlength of dentary ramus): 63 mm
Dentary (L): height (at apex of coronoid process): 146 mm
Scapula (R): height (proximodistal): 495 mm
Scapula (R): maximum width (craniocaudal) of proximal plate: 127 mm
Scapula (R): minimum width (craniocaudal) of blade: 65 mm
Scapula (R): maximum width (craniocaudal) of blade: 86 mm
Humerus (R): mediolateral width of proximal end: 78 mm
Ulna (R): length: 237 mm
Ulna (R): craniocaudal height of proximal part: 66 mm
Ulna (R): craniocaudal height of distal part: 50 mm
Radius (R): length: 198 mm
Radius (R): craniocaudal height of proximal part: 65 mm
Radius (R): craniocaudal height of distal part: 58 mm
Metacarpal II (L): length: >66 mm
Metacarpal III (R): length: 81 mm
Metacarpal IV (R): length: 85 mm
Metacarpal V (L): length: 55 mm
Metacarpal V (L): width at proximal end: 29 mm
Digit I, ungual (R): length: 58 mm
Digit II, phalanx 1 (R), length: 25 mm
Digit II, phalanx 1 (R), width at distal end: 30.5 mm
Digit II, phalanx 2 (R), length: 14 mm

Digit II, phalanx 2 (R), width at distal end: 29 mm
Digit II, ungual (R): length: 61 mm
Digit III, phalanx 1 (R), length: 20 mm
Digit III, phalanx 1 (R), width at distal end: 32 mm
Digit III, phalanx 2 (R), length: 9 mm
Digit III, ungual (R): length: 56 mm
Digit III, ungual (R): maximal width: 41 mm
Digit IV, phalanx 1 (R), length: 24 mm
Digit IV, phalanx 1 (R), width at distal end: 24 mm
Digit V, phalanx 1 (R), length: 32 mm
Digit V, phalanx 1 (R), width at distal end: 25 mm
Digit V, phalanx 2 (R), length: 16 mm
Digit V, phalanx 2 (R), width at distal end: 19 mm
Ilium (R), length: >400 mm
Ilium (R), postacetabular process, length: 100 mm
Ilium (R), postacetabular process, maximal height (taken at its cranial point): 50 mm
Tibia (L): height: 510 mm
Tibia (L): width (mediolateral) of distal end: 140 mm
Fibula (R): height: 448 mm
Fibula(R): width (craniocaudal) of proximal end: 94 mm
Fibula(R): minimal width (craniocaudal) of shaft: 27 mm

Appendix 19.2. Character List

Characters are compiled from Norman (2002, 2004), Weishampel et al. (2003), You et al. (2003a, 2003b), Horner et al. (2004), Godefroit et al. (2004, 2008), Evans and Reisz (2007), Butler et al. (2008), Sues and Averianov (2009), and Dalla Vecchia (2009).

1. Preorbital skull length: approximately 50% of total skull length (0); more than 50% of total skull length (1).
2. Premaxilla, oral margin: smooth (0); denticulate (1).
3. Premaxilla, oral margin with a "double layer" morphology consisting of an external denticles-bearing layer seen externally and an internal palatal layer of thickened bone set back slightly from the oral margin and separated from the denticulate layer by a deep sulcus bearing vascular foramina: absent (0); present (1).
4. Lateral expansion of premaxilla: narial portion of premaxilla slopes steeply from the external naris to the oral margin (0); the ventral body of the premaxilla flares laterally, so as to form a partial floor of the narial fossa, but lateral expansion less than two times of the width at postoral constriction (1); widely expanded laterally, more than two times of the width at postoral constriction (2). Character treated as ordered.
5. Reflected rim of premaxilla: absent (0); present (1).
6. Premaxillary foramen ventral to anterior margin of external nares: absent (0); present (1).
7. Premaxillary accessory narial fossa: absent (0); present (1).
8. Premaxilla–lacrimal contact: absent (0); present (1).

9. Caudal premaxillary process: short, not meeting the lateral premaxillary process posterior to external naris, external naris surrounded by both nasal and premaxilla (0); long, meeting the lateral premaxillary process behind the external naris to exclude the nasal from the external naris, nasal passage enclosed ventrally by folded, divided premaxillae (1).
10. Position of nasal cavity: nasal restricted to area rostral to braincase, nasal cavity rostromedial to orbits (0); nasals retracted caudally to lie over braincase in adults resulting in convoluted, complex narial passage and hollow crest (1).
11. Circumnarial depression: absent (0); present (1).
12. External naris: confined to the area immediately above the oral margin of the premaxilla (0); extending caudally so as to lie above the maxilla (1).
13. External naris/basal skull length ratio: 0.3 (1).
14. Caudal portion of prefrontal: oriented horizontally (0); participating in ventrolateral border of hollow crest (1).
15. Frontal, platform for nasal articulation: absent (0); present (1).
16. Frontal at orbital margin: forming part of the margin (0); excluded by prefrontal–postorbital contact (1).
17. Frontal, upward doming over braincase in adults: absent (0); present (1).
18. Supraorbital articulation: freely articulating on orbital rim (0); fused to orbital rim or absent (1).
19. Parietal, length/minimum width ratio: greater than 2 (0); less than 2 (1).
20. Parietal sagittal crest, shape: straight and level with skull roof or slightly downwarped along length (0); deepens caudally, strongly downwarped (1).
21. Parietal sagittal crest, length: short, less than ⅔ length of parietal (0); long, more than ⅔ length of parietal (1).
22. Squamosals, separation on skull roof: completely separated by the parietal (0); squamosals in broad contact with each other (1).
23. Median ramus of squamosal lower than paroccipital process (0); higher than paroccipital process (1).
24. Supraoccipital: participates in the dorsal margin of the foramen magnum (0); excluded from the dorsal margin of the foramen magnum by the paired exoccipitals (1).
25. Supraoccipital/exoccipital shelf above foramen magnum: limited (0); very extended (1).
26. Antorbital fenestra: exposed laterally (0); present as a small depression between lacrimal and maxilla (1); not exposed laterally (2). Character treated as ordered.
27. Maxilla, rostral end: single process lodged under or along the medial aspect of the premaxilla (0); second, rostrolateral process developed on the maxilla (1); development of a wide sloping maxillary shelf (2). Character treated as unordered.
28. Maxilla, dorsal process shape: low and gently rounded (0); tall and sharply peaked (1).

29. Maxilla, dorsal process position: apex of maxilla at or rostral to center (0); caudal to centre (1).
30. Maxillary foramen: absent (0); on rostrolateral maxilla (1); on dorsal maxilla along maxilla-premaxilla suture (2). Character treated as ordered.
31. Maxilla, ectopterygoid ridge: rostrocaudally short, ending at half or less length of caudal region of maxilla (0); well developed into a lateral and well demarked border continuous along caudal region of maxilla (1).
32. Maxilla–jugal suture: scarf joint (0); "finger-in-recess" (1); butt joint (2). Character treated as unordered.
33. Maxilla, number of maxillary teeth: less than 12 (0); 12–30 (1); more than 30 (2). Character treated as ordered.
34. Jugal–ectopterygoid articulation: large subtriangular ectopterygoid facet on medial side of jugal (0); small vertical ectopterygoid facet (1); absent, palatine–jugal contact enhanced (2). Character treated as ordered.
35. Jugal, expansion of rostral end below lacrimal: dorsoventrally narrow, forms little or the rostral orbital rim (0); expanded dorsoventrally in front of orbit, lacrimal pushed dorsally to lie completely above the level of maxilla, jugal forms lower portion of orbital rim (1).
36. Jugal, development of free ventral flange: absent, jugal expands gradually below infratemporal fenestra to meet quadratojugal–quadrate (0); present, jugal dorsoventrally constricted beneath infratemporal fenestra to set off flange rostral to constriction (1).
37. Jugal, development of caudal process: caudal process of jugal forms only the rostral part of the ventral margin of the infratemporal fenestra (0); extends caudally to form the ventral margin of the infratemporal fenestra (1).
38. Jugal, acute angle between postorbital bar and jugal bar: absent (0); present (1).
39. Paraquadratic foramen: present, two distinct articulation facets along margin of quadratojugal notch (0); absent, a single elongated articulation facet along margin of quadratojugal notch (1).
40. Quadrate, articular condyle: transversely expanded (0); dominated by a large hemispheric lateral condyle (1).
41. Occipital condyle, inclination: caudoventral (0); vertical (1).
42. Basipterygoid process, length: extending ventrally well below level of ventral border of occipital condyles (0); extending nearly horizontally (1).
43. Predentary, proportion: length of lateral process larger or subequal than mediolateral width of rostral margin (0); length of lateral process less than half mediolateral width of rostral margin (1).
44. Predentary, oral margin: relatively smooth (0); denticulate (1).
45. Predentary, ventral process: simple (0); bilobate (1).
46. Dentary, diastema: short, no more than width of 4 or 5 teeth (0); moderate, equal to approximately ⅕ to ¼ of tooth row (1); long, more than ⅓ of tooth row (2). Character treated as ordered.

47. Dentary ramus: parallel dorsal and ventral margins (0); deepens rostrally (1).
48. Dentary, position of coronoid process: laterally offset and dentition curves into its base (0); laterally offset and separated from dentition by a shelf (1).
49. Dentary, configuration of coronoid process: apex only slightly expanded rostrally, surangular large and forms much of caudal margin of coronoid process (0); dentary forms nearly all of rostrocaudally greatly expanded apex, surangular reduced to thin sliver along caudal margin and does not reach dorsal end of coronoid process (1).
50. Dentary, inclination of coronoid process: slightly inclined caudally or subvertical (0); inclined rostrally (1).
51. Dentary, caudal extension of tooth row: terminates even with or rostral to apex of coronoid process (0); terminates posterior to apex (1).
52. Dentary, shape of tooth row in occlusal view: bowed lingually (0); divergent caudally and convergent rostrally relative to lateral side of dentary (1); tooth row parallel with lateral side of dentary (2). Character treated as ordered.
53. Dentary, alveolar through grooves: shaped by dentary crowns (0); narrow, parallel-sided grooves (1).
54. Dentary, number of replacement teeth per tooth family: one (0); two–three (1); more than three (2). Character treated as ordered.
55. Number of tooth positions in dentary tooth row (adult specimens): less than 18 (0); 18–30 (1); more than 30 (2). Character treated as ordered.
56. Dentary, maximum number of functional teeth forming occlusal plane: one (0); two (1); three (2). Character treated as ordered.
57. Surangular foramen: present (0); absent (1).
58. Accessory surangular foramen or embayment close to the dentary suture: present (0); absent (1).
59. Angular, lateral exposure: present (0); absent (1).
60. Premaxillary teeth: 3 or more (0); absent (1).
61. Teeth roots: not cemented (0); partially cemented (1); rugose, angular-sided roots (2). Character treated as ordered.
62. Teeth, marginal denticles: single, tongue shaped (0); developed as curved, mammillated ledges (1); absent, or reduced to small papillae (2). Character treated as ordered.
63. Maxillary tooth crowns, height/width ratio at center of tooth row: ratio less than 2.4 (0); ratio at least 2.5 (1).
64. Maxillary tooth crowns, primary ridge: labial surface of maxillary crowns either smooth or exhibit an undifferentiated pattern of ridges (0); primary ridge developed (1).
65. Maxillary tooth crowns, number of accessory ridges: one primary ridge with up to three accessory ridges (0); one primary ridge with a single faint accessory ridge (1); one primary ridge, lacks accessory ridges (2). Character treated as ordered.
66. Maxillary tooth crowns, symmetry: asymmetrical, primary ridge offset from midline (0); symmetrical, primary ridge on midline (1).

67. Dentary tooth crowns, shape: broad and shieldlike, height/width ratio 3.1 (1).
68. Dentary tooth crowns, symmetry: asymmetrical, apex and primary ridge offset from midline (0); symmetrical, apex and primary ridge on midline (1)
69. Dentary tooth crowns, development of secondary ridge mesial to primary ridge: well developed, reaches the apex of the crown (0); faintly developed, does not reach the apex of the crown, absent on some teeth (1); absent or occasional (2). Character treated as ordered.
70. Dentary tooth crowns, development of tertiary ridges mesial or distal to primary ridge: at least one tertiary ridge reaches the apex of the crown (0); faintly developed, do not reach the apex of the crown (1); absent (2). Character treated as ordered.
71. Dentary tooth crowns, distal shelf at the base of the crown: absent (0), well developed but smooth (1); well developed and mammillated (2). Character treated as unordered.
72. Number of cervical vertebrae: nine or fewer (0); 10 or more (1).
73. Posterior dorsal and sacral neural spines: relatively short, less than 2.5 times centrum height (0); elongate, more than 2.5 times centrum height (1).
74. Sacrum, number of vertebrae: a maximum of 7 (0); a minimum of 8 (1).
75. Ossified hypaxial tendons in the caudal skeleton: present (0); absent (1).
76. Ossified epaxial tendons, extension: do not extend on cervical vertebrae (0); extend from cervical 10 (1).
77. Ossified epaxial tendons, organisation: longitudinally arranged (0); arranged in a double- or triple-layered lattice (1).
78. Scapula, shape of proximal region: dorsoventrally deep, acromion process directed dorsally, prominent on rostral margin of scapula, articulation extensive (0); dorsoventrally narrow (no higherer than distal scapula), acromion process projects horizontally, reflected laterally, and articulation restricted (1).
79. Coracoid, size: large, coracoid/scapula lengths more than 0.2, length of articular surface greater than length of glenoid (0); coracoid reduced in length relative to scapula, glenoid equal or longer than articulation (1).
80. Coracoid, cranioventral process: short and weakly developed (0); long, extends well below the glenoid (1).
81. Coracoid, biceps tubercle size: small (0); large and laterally projecting (1).
82. Sternal, shape: reniform (0); hatchet shaped (1).
83. Sternal, proximal plate: shorter than distal handle (0); longer than distal handle (1).
84. Proportions of humerus and scapula: length of humerus greater than or equal to length of scapula (0); scapula longer than humerus (1).
85. Humerus, deltopectoral crest shape: relatively low (0); angular and enlarged (1).

86. Carpus structure: fully ossified, with more than two small bones present, but carpals unfused (0); carpals fused into two blocks (1); reduced to no more than two small carpals (2). Character treated as unordered.
87. Manus, digit I: present, nearly parallel orientation relative to the long axis of antebrachium (0); present, diverges approximately 45 degrees from the antebrachial axis (1); absent (2). Character treated as unordered.
88. Metacarpal I, size: only slightly shorter than metacarpal II, not fused with radiale (0); less than 50% the length of metacarpal II, fused with radiale in adults (1).
89. Ungual of manual digit I: clawlike (0); spikelike, but flattened (1); spikelike and conical (2); absent (3). Character treated as unordered.
90. Unguals of manual digits II and III: clawlike (0); flattened, twisted, and hooflike (1).
91. Manual digit V: short, 2 phalanges (0); elongated, 3 or 4 phalanges (1); lost (2). Character treated as unordered.
92. Ilium, supracetabular process: small, projects only as a lateral swelling (0); large, broadly overhangs the lateral side of the ilium and usually extends at least half way down the side of ilium (1).
93. Ilium, shape of dorsal margin: regularly convex in lateral view (0); distinctly depressed over supracetabular process and dorsally bowed over base of preacetabular process (1).
94. Ilium, ischial peduncle: as a single large knob (0); formed by two small protrusions separated by a shallow depression (1).
95. Ilium, postacetabular process: tapers caudally to nearly a point, wide brevis shelf (0); postacetabular process subrectangular, no brevis shelf (1).
96. Ischium, shape of shaft in lateral view: nearly straight (0); strongly curved ventrally (1).
97. Ischium, position of obturator process: positioned beyond the proximal 25% of the length of the ischium (0); positioned within the proximal 25% (1); absent (2). Character treated as unordered.
98. Ischium, expansion of distal end: terminates without a significant increase in size (0); ischial terminus bears an expansion that is 50% larger than the adjacent ischial shaft (1).
99. Pubis, caudal ramus: terminates adjacent to distal end of ischium (0); shorter than ischium, no pubic symphysis (1).
100. Pubis, prepubic process proportion: rod shaped, wider transversely than dorsoventrally (0); transversely flattened (1).
101. Pubis, prepubic process shape in lateral view: bladelike, unexpanded distally (0); expanded distally (1).
102. Pubis, iliac peduncle: relatively small (0); has the shape of a large and dorsally directed process (1).
103. Femur, shape of fourth trochanter: pendent (0); tab shaped (1); curved, laterally compressed eminence (2). Character treated as unordered.

104. Femur, development of intercondylar extensor groove: moderately deep, groove fully open (0); deep, edges of groove meet or nearly meet cranially to enclose an extensor tunnel (1).
105. Tibia, cnemial crest: restricted to proximal head of tibia (0); extends on diaphysis (1).
106. Pedal digit 1, number of phalanges: 2 (0); 0 (1).
107. Metatarsal V: present (0); absent (1).
108. Pes, ungual phalanges: claw shaped (0); hoof shaped, but not broader than long, with prominent claw grooves retained (1); broad, short with rounded shield hooflike shape and reduced or absent claw grooves (2). Character treated as ordered.

Appendix 19.3. Data Matrix

Hypsilophodon	00000 00000 00000 00000 00?00 00000 00000 00000 00000 00000 00000 00000 00000 00000 ?0000 00000 00000 000
Zalmoxes	?0000 00000 00000 00?00 ?0?00 00000 00000 01010 10001 00000 00000 00101 00000 00000 0?000 0?000 000?0 0???? ?0000 121?0 00000 ??0
Tenontosaurus	10010 00100 01000 00000 00000 01000 000?0 00000 0?010 00000 00000 00??1 00000 00000 01000 00000 00010 00000 00000 00001 00000 0?0
Dryosaurus	00010 00100 01000 00000 00?00 01000 001?0 01000 01011 00000 00000 0?101 00010 00000 0?001 00000 0?010 000?0 ?0000 11101 00000 ?00
Camptosaurus	11010 00100 01000 00000 00000 01000 001?0 01010 01011 00000 00000 00?01 00010 00000 10001 01000 00010 11110 00000 11101 00000 010
Iguanodon	11010 00100 01000 00000 00010 01010 01100 01000 01011 00000 00001 00001 01010 00000 21001 11000 01010 11121 10000 11111 10100 111
Mantellisaurus	11010 00100 01000 00000 00010 01010 01100 01000 01011 00000 00001 00001 01010 00000 21101 11000 01010 11121 10000 11111 10100 111
Ouranosaurus	11010 00100 01000 00010 00010 01010 01100 01000 01111 11000 00001 00001 01010 00000 2110? ??000 01010 11121 ?0000 01111 10100 111
Bolong	11010 ??100 0110? ?00?? ????? 1?01? 011?0 ??0?? 00011 00000 0???1 0???1 01010 00000 210?1 0000? ???10 01111 100?0 011?? ????0 1?1
Jinzhousaurus	110?0 ??100 01000 10000 000?? 2?01? ????0 010?? ???10 ?0000 ????? 00001 ?1?11 000?? ????? ????? ????? ????? ????? ????? ????? ???
Equijubus	11010 ??100 01000 00?00 0?0?? 2?01? ?0100 01000 ???11 10?00 ??011 00101 11000 00000 ?1?01 ????? ????? ????? ?00?? ????? ????? ???
Altirhinus	110?0 00100 011?0 000?? ????? 21010 11100 11000 ??011 00100 0?0?1 00001 11011 00000

	2???? ??000 01010 01?11 ?0000 01?11 10100 ??1
Batyrosaurus	????? ????? ????0 00?00 00?10 ????? ?1?00 11?0? 1?011 00100 01111 ?0?0? 11012 00001 2???? ????? ?10?0 ???11 ????? ????? ????? ???
Probactrosaurus	11010 00?00 010?0 00?00 00010 ??010 01110 010?0 1?011 00100 01111 10?00 11012 10001 1??0? ??000 01010 ?1?11 ?0000 01111 10100 ??1
Eolambia	?1010 10?00 010?? ???00 0?0?0 2??10 01110 0?0?0 10??? 01100 0111? ?0000 11012 10012 1???? ????? ????0 ????? ?00?? 0?1?? ??10? ???
Protohadros	?1010 10?00 01000 001?? ????? 21010 01110 01010 ??011 11100 01111 ?0100 11012 10012 0???? ????? ????? ????? ????? ????? ????? ???
Shangmiaosaurus	????? ????? ????? ????? ????? ??010 021?? ????? ????? 00100 011?1 ????? 21?12 1???? 0???? ????? ????? ????? ????? ????? ????? ???
Bactrosaurus	11010 10?00 01000 00000 00010 21010 01120 01000 10011 00100 01111 11100 21012 10012 0?001 ??100 01010 ????1 ?0000 11111 11211 ??2
Levnesovia	????? ????? ???00 00?01 00010 ??010 01120 010?0 10??? 001?? ?11?1 ?110? ?1012 10012 0???? ???00 0???0 ????? ?00?? ????? ?1?1? ??2
Tethyshadros	11010 ?0100 01000 00000 0?0?? 1?000 ?22?0 01010 ???11 00101 ??11? 111?1 20111 10001 01011 01101 01010 22?31 210?1 01011 11??0 112
Telmatosaurus	11010 10?00 010?0 00?00 00010 21011 1?2?0 ?1?10 10?11 00100 11122 21100 21012 10012 0?0?? ??1?1 ??010 ????1 ????? ?1?11 1?21? ???
Brachylophosaurus	11121 11100 11100 00100 10011 21001 12221 11111 10111 20111 12122 21110 22112 11122 01011 01111 11010 22131 11111 01011 11211 112
Edmontosaurus	11121 11100 11100 00100 10011 21001 12221 11111 10111 20111 12122 21110 22112 11122 01011 01111 11010 22131 11111 01011 11211 112
Parasaurolophus	11110 00111 01011 11111 01110 22112 12221 11111 10111 10111 12122 21110 22112 11122 01111 01111 11111 22131 11111 01111 11211 112
Corythosaurus	11110 00111 01011 11111 01110 22112 12221 11111 10111 10111 12122 21110 22112 11122 01111 01111 11111 22131 11111 01111 11211 112

Appendix 19.4. Tree Description

The "describetrees" option of PAUP*4.0b10 was used to interpret character state transformations. All transformations are based on the derivative strict reduced consensus tree (see Fig. 19.12). Transformation was evaluated under accelerated transformation (ACCTRAN) and delayed transformation (DELTRAN) options; unambiguous synapomorphies are those that diagnose

a node under both ACCTRAN and DELTRAN optimizations. Node numbers refer to Figure 19.12. For simple 0–1 state changes, only the character number is given; for other state changes, the type of change is specified in parentheses. bs, bootstrap values (1,000 replicates).

Node A (bs = 77): Unambiguous: 4, 8, 12, 27, 44, 84, 100; ACCTRAN: 1, 42, 72.
Node B (Dryomorpha; bs = 85): Unambiguous: 33, 37, 45, 64, 75, 96, 97, 98; ACCTRAN: 89; DELTRAN: 42.
Node C (Ankylopollexia ; bs = 94): Unambiguous: 2, 77, 86, 87, 88, 107; ACCTRAN: 71; DELTRAN: 1, 89.
Node D (Iguanodontoidea; bs = 97): Unambiguous: 24, 29, 32, 55, 62, 82, 90, 91, 99, 101, 103, 106, 108; ACCTRAN: 71 (1 to 2); DELTRAN: 71 (0 to 2), 72.
Node E (Iguanodontidae; bs = 76): Unambiguous: 76, 89 (0 to 2).
Node F: Unambiguous: 73.
Node G (Hadrosauroidea; bs = 53): Unambiguous: 26, 42 (1 to 0), 86 (1 to 0), 96 (1 to 0); ACCTRAN: 52, 54.
Node H (bs = 60): Unambiguous: 26 (1 to 2), 61; ACCTRAN: 41; DELTRAN: 54, 62.
Node I (bs = 57): Unambiguous: 65.
Node J (bs = 57): Unambiguous: 48; ACCTRAN: 36.
Node K (bs = 75): Unambiguous: 53, 65 (1 to 2), 70; ACCTRAN: 56, 60 (1 to 0), 86 (0 to 2); DELTRAN: 41, 52.
Node L (bs = 97): Unambiguous: 34, 66; ACCTRAN: 36 (1 to 0), 39, 71 (2 to 1); DELTRAN: 56, 60 (1 to 0), 71.
Node M (bs = 94): 6, 69, 70 (1 to 2); ACCTRAN: 47, 78, 87 (1 to 2), 89 (1 to 3), 102, 105, 108 (1 to 2).
Node N (bs = 62): 58, 71 (1 to 0); ACCTRAN: 103 (1 to 2), 104.
Node O (Hadrosauridae; bs = 75): Unambiguous: 34 (1 to 2), 57, 61 (1 to 2); ACCTRAN: 47 (1 to 0); DELTRAN: 78, 102, 103 (1 to 2), 104, 105, 108 (1 to 2).
Node P (bs = 63): Unambiguous: 32 (1 to 2); ACCTRAN: 63, 74, 80, 81, 92, 94, 95, 98 (1 to 0).
Node Q (bs = 79): Unambiguous: 33 (1 to 2); ACCTRAN: 31, 50, 51, 55 (1 to 2); DELTRAN: 39, 74, 86, 87, 89, 92, 95.
Node R (bs = 62): Unambiguous: 30, 54 (1 to 2), 56 (1 to 2); ACCTRAN: 18, 36, 38, 79, 93; DELTRAN: 31, 51, 55 (1 to 2), 80.
Node S (Euhadrosauria; bs = 100): Unambiguous: 3, 35, 40, 46, 49, 52 (1 to 2), 59, 62 (1 to 2), 67, 68, 69 (1 to 2); DELTRAN: 18, 36, 38, 43, 50, 63, 79, 81, 93, 94.
Node T (Lambeosaurinae; bs = 100): Unambiguous: 6 (1 to 0), 9, 10, 14, 15, 16, 17, 19, 20, 22, 23, 27 (1 to 2), 28, 30 (1 to 2), 73, 83, 85; ACCTRAN : 98.
Node U (Hadrosaurinae; bs = 100): Unambiguous: 4 (1 to 2), 5, 7, 11, 13, 21, 25, 29 (1 to 0), 46 (1 to 2); DELTRAN: 98 (1 to 0).

Acknowledgments

The authors are particularly grateful to Bo Haichen for access to the holotype specimen of *Bolong yixianensis,* and to Sun Ge for organizing this

study. H. De Potter helped with the drawings. P. R. Bell and D. B. Norman read an earlier version of this chapter and made many helpful comments.

References

Adams, J. S., and C. L. Organ. 2005. Histologic determination of ontogenetic patterns and processes in hadrosaurian ossified tendons. Journal of Vertebrate Paleontology 25: 614–622.

Barrett, P. M., and X.-L. Wang. 2007. Basal titanosauriform (Dinosauria, Sauropoda) teeth from the Lower Cretaceous Yixian Formation of Liaoning province, China. Palaeoworld 16: 265–271.

Barrett, P. M., R. J. Butler, X.-L. Wang, and X. Xu. 2009. Cranial anatomy of the iguanodontoid ornithopod *Jinzhousaurus yangi* from the Lower Cretaceous Yixian Formation of China. Acta Palaeontologica Polonica 54: 35–48.

Brown, B. 1916. A new crested trachodont dinosaur, *Prosaurolophus maximus*. Bulletin of the American Museum of Natural History 35: 701–708.

Butler, R. J., P. Upchurch, and D. B. Norman. 2008. The phylogeny of the ornithischian dinosaurs. Journal of Systematic Palaeontology 6: 1–40.

Calvo, J. O., J. D. Porfiri, and F. E. Novas. 2007. Discovery of a new ornithopod dinosaur from the Portezuelo Formation (Upper Cretaceous), Neuquén, Patagonia, Argentina. Arquivos do Museu Nacional, Rio de Janeiro 65: 471–483.

Cifelli, R. L., J. I. Kirkland, A. Weil, A. L. Deino, and B. J. Kowallis. 1997. High-precision $^{40}Ar/^{39}Ar$ geochronology and the advent of North America's Late Cretaceous terrestrial fauna. Proceedings of the National Academy of Sciences of the United States of America 94: 11163–11167.

Cope, E. D. 1869. Synopsis of the extinct Batrachia, Reptilia and Aves of North-America. Transactions of the American Philosophical Society 14: 1–252.

Dalla Vecchia, F. M. 2009. *Tethyshadros insularis*, a new hadrosauroid dinosaur (Ornithischia) from the Upper Cretaceous of Italy. Journal of Vertebrate Paleontology 29: 1100–1116.

Dollo, L. 1888. Iguanodontidae et Camptonotidae. Comptes Rendus hebdomadaires de l'Académie des Sciences, Paris 106: 775–777.

Doré, A. G. 1991. The structural foundation and evolution of Mesozoic seaways between Europe and the Arctic. Palaeogeography, Palaeoclimatology, Palaeoecology 87: 441–492.

Evans, D. C., and R. R. Reisz. 2007. Anatomy and relationships of *Lambeosaurus magnicristatus*, a crested hadrosaurid dinosaur (Ornithischia) from the Dinosaur Park Formation. Alberta. Journal of Vertebrate Paleontology 27: 373–393.

Erickson, B. R. 1988. Notes on the postcranium of *Camptosaurus*. Scientific Publications of the Science Museum of Minnesota (n.s.) 6: 3–13.

Forster, C. A. 1990. The postcranial skeleton of the ornithopod dinosaur *Tenontosaurus tilletti*. Journal of Vertebrate Paleontology 10: 273–294.

Galton, P. M. 1970.The posture of hadrosaurian dinosaurs Journal of Paleontology 44: 464–473.

———. 1980. European Jurassic ornithopod dinosaurs of the families Hypsilophodontidae and Camptosauridae. Neues Jahrbuch für Geologie und Paläontologie, Abhandlungen 160: 73–95.

———. 1983. The cranial anatomy of *Dryosaurus*, a hypsilophodontid dinosaur from the Upper Jurassic of North America and East Africa, with a review of hypsilophodontids from the Upper Jurassic of North America. Geologica et Palaeontologica 17: 207–243.

Garrison, J. R., D. Brinkman, D. J. Nichols, P. Layer, D. Burge, and D. Thayn. 2007. A multidisciplinary study of the Lower Cretaceous Cedar Mountain Formation, Mussentuchit Wash, Utah: a determination of the paleoenvironment and paleoecology of the *Eolambia caroljonesa* dinosaur quarry. Cretaceous Research 28: 461–494.

Gates, T. A., and S. D. Sampson. 2007. A new species of *Gryposaurus* (Dinosauria: Hadrosauridae) from the late Campanian Kaiparowits Formation, southern Utah, USA. Zoological Journal of the Linnean Society 151: 351–376.

Gilmore, C. W. 1933. On the dinosaurian fauna of the Iren Dabasu Formation. Bulletin of the American Museum of natural History 67: 23–78.

Godefroit, P., Z.-M. Dong, P. Bultynck, H. Li, and L. Feng. 1998. New *Bactrosaurus* (Dinosauria: Hadrosauroidea) material from Iren Dabasu (Inner Mongolia, P.R. China). Bulletin de l'Institut royal des Sciences naturelles de Belgique, Sciences de la Terre 68 (supplement): 3–70.

Godefroit, P., V. Alifanov, and Y. L. Bolotsky. 2004. A re-appraisal of *Aralosaurus tuberiferus* (Dinosauria, Hadrosauridae) from the Late Cretaceous of Kazakhstan. Bulletin de l'Institut royal des Sciences naturelles de Belgique, Sciences de la Terre 74 (supplement): 139–154.

Godefroit, P., H. Li, and C.-Y. Shang. 2005. A new primitive hadrosauroid dinosaur from the Early Cretaceous of Inner Mongolia. Comptes rendus Palevol 4: 697–705.

Godefroit, P., S.-L Hai, T.-X. Yu, and P. Lauters. 2008. New hadrosaurid dinosaurs from the uppermost Cretaceous of northeastern China. Acta Palaeontologica Polonica 53: 47–74.

Godefroit, P., V. Codrea, and D. B. Weishampel. 2009. Osteology of *Zalmoxes shqiperorum* (Dinosauria: Ornithopoda), based on new specimens from the Upper Cretaceous of Năląţ-Vad, Romania. Geodiversitas 30: 525–553.

Head, J. J. 1998. A new species of basal hadrosaurid (Dinosauria, Ornithischia) from the Cenomanian of Texas. Journal of Vertebrate Paleontology 28: 718–738.

Horner, J. R., D. B. Weishampel, and C. A. Forster. 2004. Hadrosauridae; pp. 438–463 in D. B. Weishampel, P. Dodson, and H. Osmólska (eds.), The Dinosauria. 2nd ed. University of California Press, Berkeley.

Janensch, W. 1955. Der Ornithopode *Dysalotosaurus* der Tendaguruschichten. Palaeontographica (supplement 7) 3: 105–176.

Kirkland, J. I. 1998. A new hadrosaurid from the Upper Cedar Mountain Formation (Albian–Cenomanian Cretaceous) of Eastern Utah—the oldest known hadrosaurid (lambeosaurine?); pp. 283–295 in S. G. Lucas, J. I. Kirkland, and J. W. Estep (eds.), Lower and Middle Cretaceous terrestrial ecosystems. New Mexico Museum of Natural History and Science, Albuquerque.

Kobayashi, Y., and Y. Azuma. 2003. A new iguanodontian (Dinosauria: Ornithopoda) from the Lower Cretaceous Kitadani Formation of Fukui Prefecture, Japan. Journal of Vertebrate Paleontology 23: 166–175.

Lü, J.-C. 1997. A new Iguanodontidae (*Probactrosaurus mazongshanensis* sp. nov.) from Mazongshan Area, Gansu province, China; pp. 27–47 in Z.-M. Dong, (ed.), Sino-Japanese Silk Road dinosaur expedition. China Ocean Press, Beijing.

Lull, R. S. an N. E. Wright. 1942. Hadrosaurian dinosaurs of North America. Geological Society of America Special Papers 40: 1–242.

Marsh, O. C. 1881. Classification of the Dinosauria. American Journal of Science (ser. 3) 23: 81–86.

McDonald, A. T., J. I. Kirkland, J. Bird, and D. Deblieux. 2009. Thumb-spiked dinosaurs large, small, and strange: new information on basal iguanodonts from the Cedar Mountain Formation of Utah. Journal of Vertebrate Paleontology 29 (supplement to 3): 145A.

McDonald, A. T., D. G. Wolfe, and J. I. Kirkland. 2010. A new basal hadrosauroid (Dinosauria: Ornithopoda) from the Turonian of New Mexico. Journal of Vertebrate Paleontology 30: 799–812.

Norman, D. B. 1980. On the ornithischians dinosaur *Iguanodon bernissartensis* of Bernissart (Belgium). Mémoires de l'Institut royal des Sciences naturelles de Belgique 178: 1–103.

———. 1986. On the anatomy of *Iguanodon atherfieldensis* (Ornithischia: Ornithopoda). Bulletin de l'Institut Royal des Sciences Naturelles de Belgique, Sciences de la Terre 56: 281–372.

———. 1996. On Mongolian ornithopods (Dinosauria: Ornithischia). 1. *Iguanodon orientalis* Rozhdestvensky 1952. Zoological Journal of the Linnean Society 116: 303–313.

———. 1998. On Asian ornithopods (Dinosauria: Ornithischia). 3. A new species of iguanodontid dinosaur. Zoological Journal of the Linnean Society 122: 291–348.

———. 2002. On Asian ornithopods (Dinosauria: Ornithischia). 4. *Probactrosaurus* Rozhdestvensky, 1966. Zoological Journal of the Linnean Society 136: 113–144.

———. 2004. Basal Iguanodontia; pp. 413–437 in D. B. Weishampel, P. Dodson, and H. Osmólska (eds.), The Dinosauria. 2nd ed. University of California Press, Berkeley.

Ostrom, J. H. 1961. Cranial morphology of the hadrosaurian dinosaurs of North America. Bulletin of the American Museum of Natural History 122: 33–186.

———. 1970. Stratigraphy and paleontology of the Cloverly Formation (Lower Cretaceous) of the Bighorn Basin area, Wyoming and Montana. Bulletin, Peabody Museum of Natural History 30: 1–234.

Owen, R. 1842. Report on British Fossil Reptiles. Part 2. Report of the British Association for the Advancement of Science (Plymouth) 11: 60–204.

Parks, W. A. 1920. The osteology of the trachodont dinosaur *Kritosaurus incurvimanus*. University of Toronto Studies, Geological Series 11: 1–74.

Prieto-Marquez, A. 2007. Postcranial osteology of the hadrosaurid dinosaur *Brachylophosaurus canadensis* from the Late Cretaceous of Montana; pp. 91–115 in K. Carpenter, (ed.), Horns and beaks: ceratopsian and ornithopod dinosaurs. Indiana University Press, Bloomington.

Ruiz-Omeñaca, J.-I, Pereda-Suberbiola, X., and Galton, P. M. 2007. *Callovosaurus leedsi*, the earliest dryosaurid dinosaur (Ornithischia: Euornithopoda) from the Middle Jurassic of England; pp. 3–16 in K. Carpenter (ed.), Horns and beaks: ceratopsian and ornithopod dinosaurs. Indiana University Press, Bloomington.

Russell, D. A. 1993. The role of Central Asia in dinosaurian biogeography. Canadian Journal of Earth Sciences 30: 2002–2012.

Seeley, H. G. 1887. On the classification of the fossil animals commonly called Dinosauria. Proceedings of the Royal Society of London 43: 165–171.

Sereno, P. C. 1986. Phylogeny of the bird-hipped dinosaurs (Order Ornithischia). National Geographic Society Research 2: 234–256.

———. 1997. The origin and evolution of dinosaurs. Annual Review of Earth and Planetary Sciences 25: 435–489.

———. 1998. A rationale for phylogenetic definitions, with application to the higher-level taxonomy of Dinosauria. Neues Jahrbuch für Geologie und Paläontologie. Abhandlungen 210: 41–83.

Smith, P. E., N. M. Evensen, D. York, M.-M. Chang, F. Jin, J.-L. Li, S. L. Cumbaa, and D. A. Russell. 1995. Dates and rates in ancient lakes: $^{40}Ar/^{39}Ar$ evidence for an Early Cretaceous age for the Jehol Group, northeast China. Canadian Journal of Earth Sciences 32: 1426–1431.

Sues, H.-D., and A. Averianov. 2009. A new basal hadrosauroid dinosaur from the Late Cretaceous of Uzbekistan and the early radiation of duck-billed dinosaurs. Proceedings of the Royal Society B 276: 2549–2555.

Swisher, C. C., III, Y.-Q. Wang, X.-L. Wang, X. Xu, and Y. Wang. 1999. Cretaceous age for the feathered dinosaurs of Liaoning, China. Nature 400: 58–61.

Swisher C. C., III, X. Wang, Z. Zhou, Y. Wang, F. Jin, J. Zhang, X. Xu, F. Zhang, and Y. Wang. 2002. Further support for a Cretaceous age for the feathered-dinosaur beds of Liaoning, China: new $^{40}Ar/^{39}Ar$ dating of the Yixian and Tuchengzi formations. Chinese Science Bulletin 47: 135–138

Swofford, D. L. 2000. Phylogenetic analysis using parsimony (and other methods).

Version 4.0b10. Sinauer Associates, Sunderland, Mass., 40 pp.
Taquet, P. 1976. Géologie et paléontologie du gisement de Gadoufaoua (Aptien du Niger). Cahiers de Paléontologie, CNRS, Paris.
Taquet P., and D. A. Russell. 1999. A. massively-constructed iguanodont from Gadoufaoua, Lower Cretaceous of Niger. Annales de Paléontologie 85: 85–96.
Wang, X.-L., and X. Xu. 2001. A new iguanodontid (*Jinzhousaurus yangi* gen. et sp. nov.) from the Yixian Formation of western Liaoning, China. Chinese Science Bulletin 46: 419–423.
Wang, X.-L., H.-L. You, Q. Meng, C.-L. Gao, X.-D. Cheng, and J.-Y. Liu. 2007. *Dongbeititan dongi*, the first sauropod dinosaur from the Lower Cretaceous Jehol Group of western Liaoning province, China. Acta Geologica Sinica 81: 911–916.
Wang, X.-L., R. Pan, R. J. Butler, and P. M. Barrett. 2011. The postcranial skeleton of the iguanodontian ornithopod *Jinzhousaurus yangi* from the Lower Cretaceous Yixian Formation of western Liaoning, China. Earth and Environmental Science Transactions of the Royal Society of Edinburgh 101: 135–159.
Weishampel, D. B., D. B. Norman, and D. Grigorescu. 1993. *Telmatosaurus transsylvanicus* from the Late Cretaceous of Romania: the most basal hadrosaurid dinosaur. Palaeontology 36: 361–385.
Weishampel, D. B., C.-M. Jianu, Z. Csiki, and D. B. Norman. 2003. Osteology and phylogeny of *Zalmoxes* (n.g.), an unusual euornithopod dinosaur from the latest Cretaceous of Romania. Journal of Systematic Palaeontology 1: 65–123.
Winkler, D. A., P. A. Murry, and L. L. Jacobs. 1997. A new species of *Tenontosaurus* (Dinosauria: Ornithopoda) from the Early Cretaceous of Texas. Journal of Vertebrate Paleontology 17: 330–348.
Wu, W.-H., P. Godefroit, and D.-Y. Hu. 2010. A new iguanodontoid dinosaur (*Bolong yixianensis* gen. et sp. nov.) from the Yixian Formation of western Liaoning, China. Geology and Resources 19: 127–133.
Xu, X., and M. A. Norell. 2006. Non-avian dinosaur fossils from the Lower Cretaceous Jehol Group of western Liaoning, China. Geological Journal 4: 419–437.
Xu, X., X.-Y. Zhao, J.-C. Lü, W.-B. Huang, and Z.-M. Dong. 2000. A new iguanodontian from the Sangping Formation of Neixiang, Henan and its stratigraphical implications. Vertebrata PalAsiatica 38: 176–191.
You, H.-L., and D.-Q. Li. 2009. A new basal hadrosauriform dinosaur (Ornithischia: Iguanodontia) from the Early Cretaceous of northwestern China. Canadian Journal of Earth Sciences 46: 949–957.
You, H.-L., Q. Ji, J.-L. Li, and Y.-X. Li. 2003a. A new hadrosauroid dinosaur from the Mid-Cretaceous of Liaoning, China. Acta Geologica Sinica 77: 148–154.
You, H.-L., Z.-X. Luo, N. H. Shubin, L. M. Witmer, Z.-L. Tang, and F. Tang. 2003b. The earliest-known duck-billed dinosaur from deposits of late Early Cretaceous age in northwest China and hadrosaur evolution. Cretaceous Research 24: 347–355.
You, H.-L., Q. Ji, and D.-Q. Li. 2005. *Lanzhousaurus magnidens* gen. et sp. nov. from Gansu province, China: the largest-toothed herbivorous dinosaur in the world. Geological Bulletin of China 24: 785–794.
Zhou, Z.-H. 2006. Evolutionary radiation of the Jehol Biota: chronological and ecological perspectives. Geological Journal 41: 377–393.